Further Mathematical Biology

Lecture Notes

Prof Ruth E Baker

Michaelmas Term 2023

Abstract

These lecture notes have been written to accompany the Part B course *Further Mathematical Biology*. They are based heavily on lecture notes and material originally developed by many members of the department, including myself, Professors Philip Maini, Helen Byrne, Eamonn Gaffney, Jon Chapman and Andrew Fowler.

If you have not taken the Part A short option *Mathematical Modelling in Biology*, you are encouraged to work through the lecture notes. In particular you should focus on the sections that explore continuous-time models for single and interacting species.

General suggested reading material is listed on the course webpages, and more specific references can be found within each chapter.

Ruth Baker, MT 2023.

Contents

Chapter 1

Introduction

We will show that many phenomena in ecology, biology, biochemistry and medicine can be modelled mathematically. We will learn how to formulate mathematical models of biological processes, how to analyse them using a range of techniques from applied mathematics, and then how to relate the outcomes of our mathematical analysis to the real-world system we are studying. We will focus initially on systems where spatial variation is either absent or, at least, not important. In such cases only the temporal evolution needs to be described, and typically this is done using differential equations that describe how the concentrations or densities evolve over time. We will study how to build and analyse these models in order to extract useful information from them. We will then consider examples where there is explicit spatial variation, and so we need to build models that incorporate spatial effects. In ecological and biological applications the main physical phenomenon governing spatial variation is typically, but not exclusively, diffusion. Thus many models use systems of parabolic partial differential equations to describe biological mechanisms, again in terms of the evolution of concentration or density. We will study how to build and analyse models in this context. Finally, we will explore how to connect these macroscale models to more detailed models that take into account the behaviour of individuals within a system. In particular we will draw examples from:

- physiology;
- infectious disease epidemics;
- biological pattern formation;
- cell cycle dynamics and tissue growth;
- tumour growth.

The main references for this lecture course will be:

- J. D. Murray, *Mathematical Biology, Volume I: An Introduction*, 3rd Edition (Springer, 2002);
- J. D. Murray, *Mathematical Biology, Volume II: Spatial Models and Biomedical Applications*, 3rd edition (Springer, 2003);
- L. Edelstein-Keshet, *Mathematical Models in Biology* (SIAM, 2005).

Other useful references include (but are no means compulsory):

- J. Keener and J. Sneyd, *Mathematical Physiology*, First Edition (Springer, 1998);
- N. F. Britton, *Essential Mathematical Biology* (Springer, 2003).

Additional references that provide interesting, related reading are listed within the text.

Chapter 2

Delay models

In the Part A *Mathematical Modelling in Biology* course, we studied models of the form

$$\frac{\mathrm{d}N}{\mathrm{d}t} = f\left(N(t)\right), \tag{2.1}$$

so that the rate of change of the population depends on the current population size. However, this is not always realistic. For example, offspring are not produced instantaneously – the gestation period can last a significant length of time – and usually new offspring take some time to mature to adulthood and become capable of reproduction. This means that, for example, the birth rate in a population may depend on the size of the population some time ago. Delays can be incorporated using the framework of *delay differential equation* models of the form

$$\frac{\mathrm{d}N}{\mathrm{d}t} = f\left(N(t), N(t-T)\right), \tag{2.2}$$

where $T > 0$ is the delay.

In this chapter we will develop and analyse delay models and show how they can be used to study population dynamics and physiological processes.

2.1 The delayed logistic model

A commonly used example of a delay model is the delayed logistic model:

$$\frac{\mathrm{d}N}{\mathrm{d}t} = rN(t)\left(1 - \frac{N(t-T)}{K}\right), \tag{2.3}$$

where $r > 0$ is the intrinsic growth rate and $K > 0$ is the carrying capacity. Note that to be able to compute the solution we need to specify $N(t)$ for $-T \leq t \leq 0$.

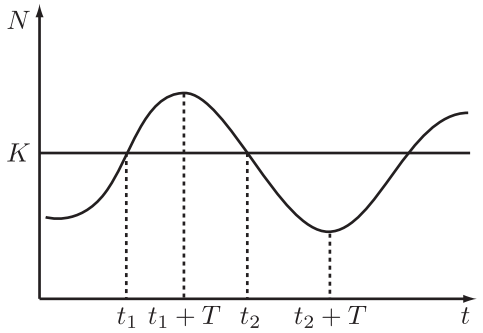

Figure 2.1: Schematic of the oscillatory nature of solutions.

We can get some idea of the possible behaviour of the model using heuristic reasoning (see Figure 2.1). Suppose that at $t = t_1$, $N(t_1) = K$, and that for some time $t < t_1$, $N(t - T) < K$. Then at this time t, $\mathrm{d}N/\mathrm{d}t > 0$ and so $N(t)$ is increasing. Also, when $t = t_1 + T$, $\mathrm{d}N/\mathrm{d}t = 0$. For $t_1 + T < t < t_2$, $\mathrm{d}N/\mathrm{d}t < 0$ and so $N(t)$ decreases until $t = t_2 + T$ when $\mathrm{d}N/\mathrm{d}t = 0$ again. Therefore there is the possibility of oscillatory behaviour. We expect that the period of these limit cycle solutions will be approximately $4T$.

Equation (2.3) can exhibit *stable limit cycle* periodic solutions for a large range of values of rT. This means that if t_p is the period then $N(t + t_p) = N(t)$, and if a perturbation is imposed then the solution returns to the original periodic behaviour as $t \to \infty$ (although a *phase shift* may occur).

Note. Single species populations models without delays cannot exhibit limit cycle behaviour. To see this, suppose that such a model as Equation (2.1) has a periodic solution with period t_p. Then

$$\int_t^{t+t_p} \left(\frac{\mathrm{d}N}{\mathrm{d}t}\right)^2 \mathrm{d}t = \int_t^{t+t_p} f(N)\frac{\mathrm{d}N}{\mathrm{d}t}\mathrm{d}t = \int_{N(t)}^{N(t+t_p)} f(N)\,\mathrm{d}N = 0, \tag{2.4}$$

since $N(t + t_p) = N(t)$. Since the left-hand-most term in the above equation is non-negative this means that $\mathrm{d}N/\mathrm{d}t \equiv 0$ and hence we have a contradiction.

2.1.1 Linear analysis of delayed population models

We will use the delayed logistic model as an example, and investigate the linear stability of the steady states $N = K$ and $N = 0$. We non-dimensionalise as before by letting $N = KN^*$, $t = t^*/r$ and $T = T^*/r$ to give (dropping the asterisks for notational convenience):

$$\frac{\mathrm{d}N}{\mathrm{d}t} = N(t)\left[1 - N(t - T)\right]. \tag{2.5}$$

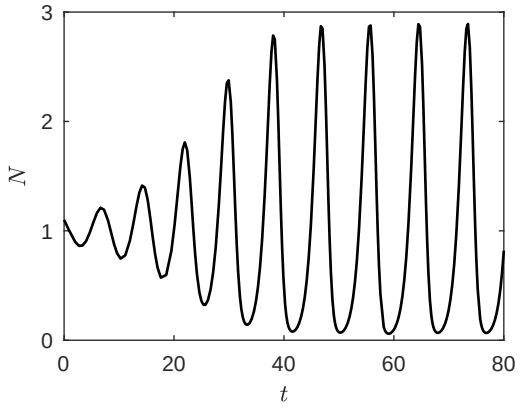

Figure 2.2: Dynamics of the non-dimensional delayed logistic model with $T = 2$ and $N(t) = 1$ for $-2 \leq t \leq 0$.

The steady states are $N = 0$ and $N = 1$ and, as for the non-delayed logistic equation studied in the Part A *Mathematical Modelling in Biology* course, we will investigate the linear stability of the steady state $N = 1$.

First we linearise about the steady state by writing $N(t) = 1 + n(t)$ so that

$$\frac{\mathrm{d}n(t)}{\mathrm{d}t} \approx -n(t - T). \tag{2.6}$$

Seeking solutions of the form $n(t) = n(0)\exp(\lambda t)$ gives

$$\lambda = -e^{-\lambda T}. \tag{2.7}$$

This is a transcendental equation for λ that has infinitely many roots. To determine the linear stability we require an understanding of whether there are solutions with $Re(\lambda) > 0$. To investigate, we let $\lambda = \mu + i\,\omega$ and explore the values of the delay, T, for which μ is positive or negative.

Substituting into Equation (2.7) we have equations that define μ and ω in terms of T:

$$\mu = -e^{-\mu T}\cos(\omega T); \tag{2.8}$$

$$\omega = e^{-\mu T}\sin(\omega T). \tag{2.9}$$

We would like to determine the range of values of T such that $\mu < 0$. Suppose first that $\omega = 0$ so that λ is real. Then Equation (2.9) is satisfied, and Equation (2.8) gives $\mu = -\exp(\mu t)$ which has no positive roots. Suppose now that $\omega \neq 0$. If ω is a solution then so is $-\omega$, so without loss of generality let $\omega > 0$. From Equation (2.8), $\mu < 0$ (stability) requires $0 < \omega T < \pi/2$.

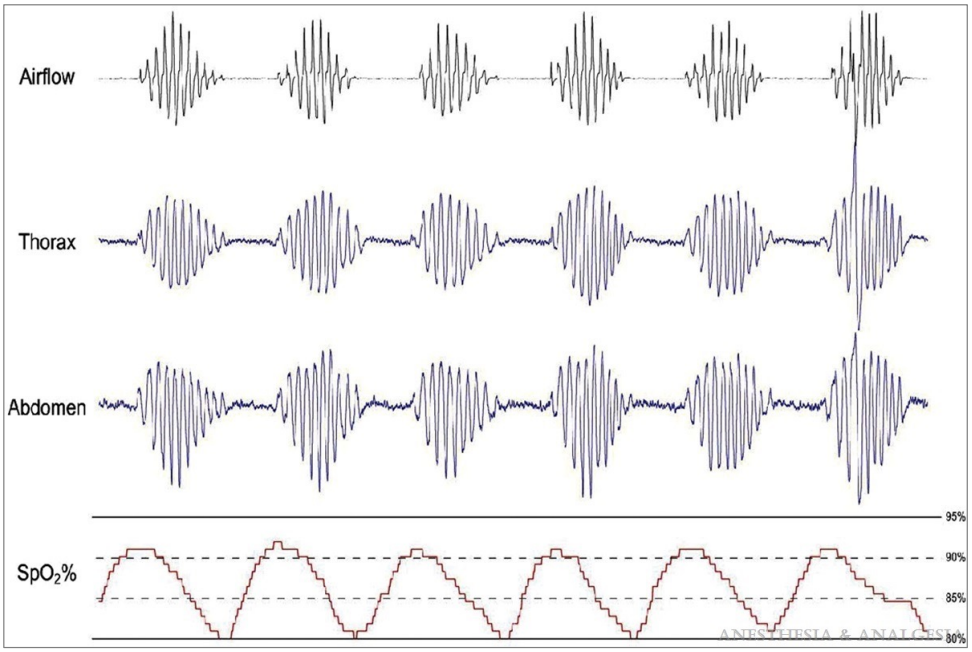

Figure 2.3: Illustration of Cheyne–Stokes breathing. Taken from Correa *et al. Anesthesia and Analgesia* 120(6):1273–1285 (2015).

We are interested in understanding when, as we increase the value of T, $\mu(T)$ first becomes positive. As T increases from zero, μ first becomes zero when $\omega T = \pi/2$, and at this point (from Equation (2.9)) we see that $\omega = 1$. Hence the steady state first becomes unstable at the bifurcation point $T = T_c = \pi/2$ *i.e.* $N = 1$ is stable for $0 < T < \pi/2$.

Going back to the dimensional model, this means that the steady state $N(t) = K$ is stable if $0 < rT < \pi/2$ and unstable for $rT > \pi/2$, and we anticipate stable limit cycle behaviour in the latter case. Figure 2.2 illustrates the stable limit cycle behaviour that can arise in the delayed logistic model. We see oscillations that gradually increase to have stable amplitude, with period approximately $4T$.

2.2 Cheyne–Stokes respiration

Cheyne–Stokes respiration is an abnormal breathing pattern that is characterised by a series of progressively deeper, and sometimes faster, breaths that are followed by gradually shallower breaths that result in a temporary stop in breathing (called apnea). Each cycle usually lasts between 30 seconds and two minutes, and they are associated with changing serum pressures of oxygen and carbon dioxide. Figure 2.3 illustrates this phenomenon.

To make progress in understanding how Cheyne–Stokes respiration arises, we will build a mathematical model. We denote the breath volume, also known as the ventilation, as $V(t)$.

The level of arterial carbon dioxide, $C(t)$, is monitored by receptors that, in turn, determine the ventilation, $V(t)$. The response to changing carbon dioxide levels is not instantaneous, and this introduces a delay, t_0, into the breathing control system that represents the time between oxygenation of the blood in the lungs and the monitoring of levels in the brain.

A good model for how ventilation levels depend on the levels of arterial carbon dioxide is given by the Hill function

$$V(t) = V_{\max}\frac{C^m(t-t_0)}{A^m + C^m(t-t_0)}, \tag{2.10}$$

where $V_{\max} > 0$ is the maximum possible ventilation and the positive constants A and m are parameters determined from experimental data. We make the assumption that carbon dioxide is produced at a constant rate, $P > 0$, in the body, and that it is removed at a rate proportional to the product of the carbon dioxide levels and the ventilation.

The dynamics of carbon dioxide levels are then given by the following delay differential equation:

$$\frac{\mathrm{d}C}{\mathrm{d}t} = P - BC(t)V(t) = P - BV_{\max}C(t)\frac{C^m(t-t_0)}{A^m + C^m(t-t_0)}, \tag{2.11}$$

where $B > 0$ is the rate of carbon dioxide removal. The system is closed by specifying $C(t)$ for $-t_0 \leq t \leq 0$.

We can non-dimensionalise by setting

$$C(t) = Ac(\tau), \qquad V(t) = V_{\max}v(\tau), \qquad t = \frac{A}{P}\tau, \qquad t_0 = \frac{A}{P}\tau_0, \tag{2.12}$$

so that

$$\frac{\mathrm{d}c}{\mathrm{d}\tau} = 1 - ac(\tau)v(\tau) = 1 - ac(\tau)\frac{c^m(\tau-\tau_0)}{1 + c^m(\tau-\tau_0)}, \tag{2.13}$$

where

$$a = \frac{ABV_{\max}}{P} \qquad \text{and} \qquad v(\tau) = \frac{c^m(\tau-\tau_0)}{1 + c^m(\tau-\tau_0)}. \tag{2.14}$$

The steady states, c_*, satisfy

$$\frac{1}{c_*} = av(c_*) = a\frac{c_*^m}{1 + c_*^m}. \tag{2.15}$$

To see that the steady state exists, and that it is unique, we can plot

$$f_1(c) = \frac{1}{c} \qquad \text{and} \qquad f_2(c) = \frac{ac^m}{1 + c^m}. \tag{2.16}$$

2.2.1 Linear stability analysis

The ventilation, $V(t)$, should be constant for healthy individuals at rest. This is not the case for Cheyne–Stokes respiration. We will use linear stability analysis to explore the stability of the steady state, paying careful attention to explore the possibility that the model might exhibit oscillatory solutions (as consistent with Cheyne–Stokes respiration).

First, let

$$v_* = \frac{c_*^m}{1 + c_*^m}, \tag{2.17}$$

and

$$c(\tau) = c_* + \epsilon c_1(\tau) + \ldots, \tag{2.18}$$

so that

$$v(c) = v(c_* + \epsilon c_1(\tau - \tau_0) + \ldots) = v_* + \epsilon v'(c_*)c_1(\tau - \tau_0) + \mathcal{O}(\epsilon^2), \tag{2.19}$$

where, with some abuse of notation, we have

$$v'(c_*) = \left.\frac{\mathrm{d}v}{\mathrm{d}c}\right|_{c=c_*}. \tag{2.20}$$

Note that $v'(c_*) > 0$ (see sketch showing existence and uniqueness of the steady state).

Substituting into Equation (2.13) gives the linearised equation

$$\frac{\mathrm{d}c_1}{\mathrm{d}\tau} = -av_*c_1(\tau) - ac_*v'(c_*)c_1(\tau - \tau_0). \tag{2.21}$$

We seek solutions of the form $c_1(\tau) = c_1(0)e^{\lambda\tau}$, which gives a transcendental equation for λ,

$$\lambda = -a\left[v_* + c_*v'(c_*)e^{-\lambda\tau_0}\right]. \tag{2.22}$$

In the case of no delay, $\tau_0 = 0$, we have

$$\lambda = -a\left[v_* + c_*v'(c_*)\right] < 0, \tag{2.23}$$

and so the steady state is stable. Further, for all $\lambda \in \mathbb{R}$ we have $\lambda < 0$ and the steady state is stable.

Now suppose that $\lambda = \mu + i\omega$ with $\omega \neq 0$. Then

$$\lambda = \mu + i\omega = -a\left[v_* + c_*v'(c_*)e^{-(\mu+i\omega)\tau_0}\right]. \tag{2.24}$$

Equating real and imaginary parts gives

$$\begin{aligned} \mu &= -a\left[v_* + c_* v'(c_*) e^{-\mu\tau_0}\cos(\omega\tau_0)\right] && (2.25)\\ &= -\alpha - \beta e^{-\mu\tau_0}\cos(\omega\tau_0), \\ \omega &= a c_* v'(c_*) e^{-\mu\tau_0}\sin(\omega\tau_0) && (2.26)\\ &= \beta e^{-\mu\tau_0}\sin(\omega\tau_0), \end{aligned}$$

where

$$\alpha = a v_* > 0 \qquad \text{and} \qquad \beta = a c_* v'(c_*) > 0. \tag{2.27}$$

A bifurcation to oscillating solutions occurs at $\mu = 0$, and here

$$\cos(\omega\tau_0) = -\frac{\alpha}{\beta}, \tag{2.28}$$

$$\sin(\omega\tau_0) = \frac{\omega}{\beta}. \tag{2.29}$$

Combining these equations gives

$$\omega^2 = \beta^2 - \alpha^2. \tag{2.30}$$

Equation (2.28) has an infinite number of roots when $\alpha < \beta$. Consider the smallest of these (in absolute value). We see that the conditions for a bifurcation at $\tau_0 = \tau_0^*$ are

$$\omega\tau_0^* = \pi - \cos^{-1}\left(\frac{\alpha}{\beta}\right) \qquad \text{and} \qquad \omega^2 = \beta^2 - \alpha^2. \tag{2.31}$$

If these equations cannot be satisfied then no bifurcation can occur. On the other hand, if they are satisfied then we see that the bifurcation takes place at a critical value of the delay, τ_0, given by

$$\tau_0^* = \frac{\pi - \cos^{-1}\left(\frac{\alpha}{\beta}\right)}{\sqrt{\beta^2 - \alpha^2}}. \tag{2.32}$$

In summary, for small values of the delay, τ_0, the steady state, c_*, is stable, and as τ_0 is increased past τ_0^* the system undergoes a bifurcation so that c_* becomes unstable.

Since the eigenvalues are complex when we have an instability, this means that we have oscillatory behaviour. In fact, after the onset of instability, the system moves towards an oscillatory solution. If we suppose that the period of the final periodic solution is the same as that of the period of the oscillatory growth regime, then the period of the oscillations can be determined by linear stability analysis.

2.2.2 Physiologically relevant parameter values

We now explore whether the steady state is likely to become unstable for physiologically relevant parameter values. We will write, again with some abuse of notation,

$$V_* = V(C_*) = V_{\max}\frac{C_*^m}{A^m + C_*^m}. \tag{2.33}$$

Typical estimates for the parameters are (note that the concentration of gas in the blood is measured in terms of the partial pressure it sustains)

$$C_* = 40\,\text{mmHg}, \qquad P = 6\,\text{mmHg}\,\text{min}^{-1}, \qquad t_0 = 0.25\,\text{min}, \qquad V_* = 7\,\text{L}\,\text{min}^{-1},$$

$$V'(C_*) = 4\,\text{L}\,\text{min}^{-1}\,\text{mmHg}^{-1}, \qquad B = \frac{P}{C_* V_*} \approx 0.021\,\text{L}^{-1}\,\text{min}^{-1}.$$

First, we note that

$$\omega\tau_0 = \pi - \cos^{-1}\left(\frac{\alpha}{\beta}\right) = \pi - \cos^{-1}\left(\frac{V_*}{C_* V'(C_*)}\right) = \pi - \cos^{-1}\left(\frac{7}{4\times 40}\right) \approx \frac{\pi}{2}, \tag{2.34}$$

and

$$\alpha = a v_* = a v(c_*) = \frac{AB}{P} V_* \qquad \text{and} \qquad \beta = c_* v'(c_*) = \frac{AB}{P} C_* V'(C_*). \tag{2.35}$$

Recall that the condition for stability of the steady state c_* is

$$\tau_0 < \frac{\pi - \cos^{-1}\left(\frac{\alpha}{\beta}\right)}{\sqrt{\beta^2 - \alpha^2}}. \tag{2.36}$$

As such, in dimensional terms the condition for stability of the steady state C_* is

$$\frac{Pt_0}{A}\left\{\left(\frac{AB}{P}\right)^2\left[C_*^2 V'(C_*)^2 - V_*^2\right]\right\}^{1/2} \lessapprox \frac{\pi}{2}, \tag{2.37}$$

or

$$Pt_0\left(\frac{1}{V_*^2}V'(C_*)^2 - \frac{1}{C_*^2}\right)^{1/2} \lessapprox \frac{\pi}{2}, \tag{2.38}$$

where we have used the fact that $P - BC_*V_* = 0$ (see Equation (2.11)).

Given the stated parameter values, the first term on the left-hand side of Equation (2.38) is much larger than the second. As such, we ignore the second term and the constraint required for

stability becomes

$$V'(C_*) \lessapprox \frac{\pi V_*}{2Pt_0}. \tag{2.39}$$

This means that the steady state becomes unstable if the gradient of the ventilation function at the steady state becomes too large. The biological interpretation of this result is that periodic changes in ventilation (and hence Cheyne–Stokes breathing) can arise if the physiological response to changes in carbon dioxide levels becomes too abrupt.

We have

$$\text{non-dimensional period} = \frac{2\pi}{\omega} \approx 4\tau_0, \tag{2.40}$$

where we have used the fact that $\omega\tau_0 \approx \pi/2$. Translating this result back to dimensional quantities, we see that the dimensional period is about $4t_0 \approx 1\,\text{min}$, which is in agreement with observations.

Suggested reading.

- J. D. Murray, *Mathematical Biology, Volume I* – Chapter 1.
- F. A. Rihan, *Delay Equations and Applications to Biology.* Available at `https://link.springer.com/book/10.1007\%2F978-981-16-0626-7`
- M. C. Mackey and L. Glass. Oscillation and chaos in physiological control systems. *Science* 197(4300):287–289. Available at `https://www.jstor.org/stable/1744526`

Chapter 3

Age-structured models

The simplest models of population dynamics treat all individuals as identical. Consider, for example, the logistic growth law. More sophisticated models decompose the population into distinct subgroups. For example, SIR models of diseases such as measles, chicken pox and HIV/AIDS typically decompose the population into three subgroups (susceptibles, infectives and recovereds), and time-dependent ordinary differential equations describe their evolution. In practice, however, many processes involved in population growth and/or disease spread depend on age: young and old individuals may have higher mortality rates and be more susceptible to a disease; only individuals of a certain age may be able to produce offspring; school children who frequently come into contact with each other may play a stronger role in disease transmission than other age-groups. Figure 3.1 shows examples of the population age distribution for Germany, Mexico and Uganda, and illustrates how they are likely to change by 2050.

In this chapter we will develop and analyse age-structured population models and show how they can be used to study population dynamics, epidemics and cell-cycle dynamics.

3.1 Simple birth-death population models with age structure

We denote by $n(t, a)$ the number of individuals of age a at time t, and suppose that the population changes only through births and deaths. We introduce $b = b(a)$ as the birth rate of individuals of age a, and $\mu = \mu(a)$ as the death rate of individuals of age a.

Possible functional forms for the birth and death rates $b(a)$ and $\mu(a)$ are

$$\mu(a) = \mu_{\max}\left(1 - \frac{A_{\min} a}{A_{\min}^2 + a^2}\right) \quad \text{and} \quad b(a) = \begin{cases} b & \text{for } a_L < a < a_R, \\ 0 & \text{otherwise.} \end{cases} \tag{3.1}$$

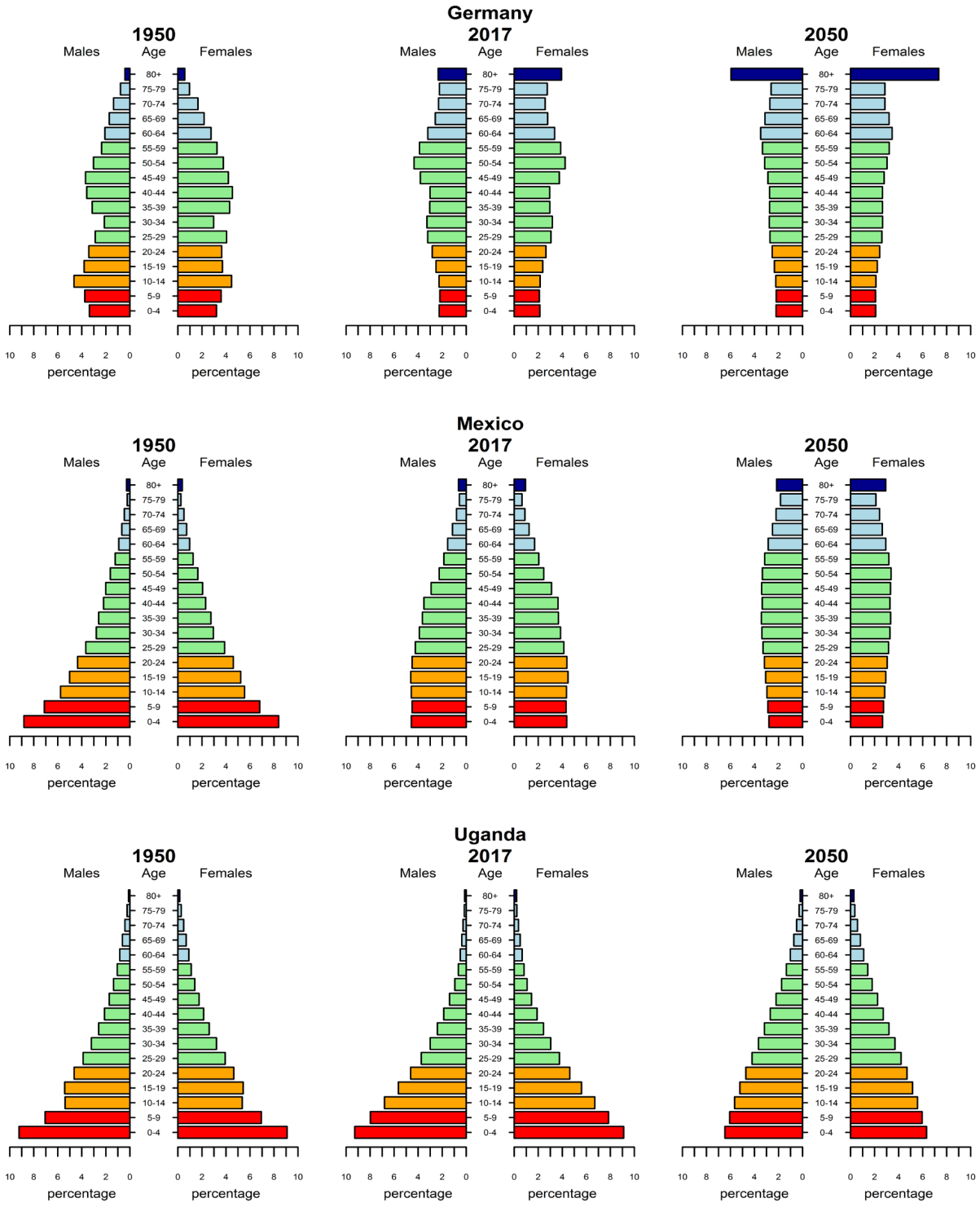

Figure 3.1: Histograms highlighting differences in the age distribution of males and females in Germany, Mexico and Uganda, and how they are likely to change by 2050 [15].

3.1.1 Von Foerster's equation

To build a model of how the population evolves in time we use the principle of mass conservation. First, we note that the birth rate contributes only to the number of newborns, $n(t, a = 0)$. In addition, over a given period of time only death and ageing will alter the number of individuals of a given age $a > 0$. We deduce that, over the short interval of time δt,

$$\mathrm{d}n(t,a) = \frac{\partial n}{\partial t}\delta t + \frac{\partial n}{\partial a}\delta a = -\mu(a)n(t,a)\delta t. \tag{3.2}$$

Dividing through by δt and noting that, since a is chronological age,

$$\lim_{\delta t \to 0} \frac{\delta a}{\delta t} = \frac{\mathrm{d}a}{\mathrm{d}t} = 1, \tag{3.3}$$

we deduce that $n(t, a)$ satisfies the following linear partial differential equation:

$$\frac{\partial n}{\partial t} + \frac{\partial n}{\partial a} = -\mu(a)n, \tag{3.4}$$

which is known as **von Foerster's equation**.

To solve Equation (3.4), we impose the following initial and boundary conditions:

$$n(0,a) = f(a), \quad \text{initial age-distribution of population;} \tag{3.5}$$

$$n(t,0) = \int_0^\infty b(a)n(t,a)\mathrm{d}a, \quad \text{birth rate of population.} \tag{3.6}$$

We use the method of characteristics to solve Equations (3.4)–(3.6). The characteristic curves satisfy

$$\frac{\mathrm{d}a}{\mathrm{d}t} = 1 \qquad \text{on which} \qquad \frac{\mathrm{d}n}{\mathrm{d}t} = -\mu n. \tag{3.7}$$

From Figure 3.2 it is clear that:

- characteristic curves for which $0 < t < a$ emanate from the initial data (where $t = 0$);
- characteristics for which $0 < a < t$ emanate from the boundary conditions (at $a = 0$).

Since information from the boundary and initial conditions propagates along characteristics, we deduce that the solution will have different forms in $0 < t < a$ and $0 < a < t$. We construct these solutions below.

Using Figure 3.2, we see that the characteristic curves are given by

$$a = \begin{cases} t + a_0 & \text{for } a > t, \\ t - t_0 & \text{for } a < t, \end{cases} \tag{3.8}$$

where a_0 represents the initial age of an individual who has age $a > t$ at time t, and t_0 represents the time at which an individual of age $0 < a < t$ was born.

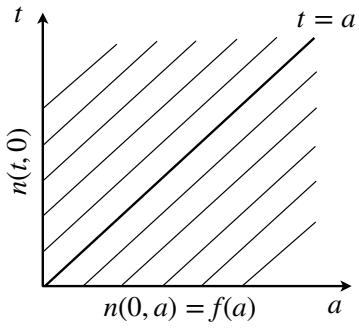

Figure 3.2: The characteristic curves associated with von Foerster's equation.

Region 1. In this region $0 < t < a$ and so we have

$$\frac{\partial n}{\partial t} + \frac{\partial n}{\partial a} = -\mu(a)n, \qquad n(0, a) = f(a), \tag{3.9}$$

Hence

$$\begin{aligned} a &= t + a_0, & (3.10)\\ \frac{\mathrm{d}n}{\mathrm{d}t} &= -\mu n, & (3.11)\\ n(0, a_0) &= f(a_0). & (3.12) \end{aligned}$$

so that

$$n(t, a) = n(0, a_0) \exp\left\{ -\int_{a_0}^{a} \mu(\theta)\mathrm{d}\theta \right\}. \tag{3.13}$$

Since $a_0 = a - t$ along characteristic curves, we have

$$n(t, a) = f(a - t) \exp\left\{ -\int_{a-t}^{a} \mu(\theta)\mathrm{d}\theta \right\}. \tag{3.14}$$

Region 2. In this region $0 < a < t$ and so we have

$$\frac{\partial n}{\partial t} + \frac{\partial n}{\partial a} = -\mu(a)n, \qquad n(t, 0) = \int_0^\infty b(a)n(t, a)\mathrm{d}a. \tag{3.15}$$

Hence

$$\begin{aligned} a &= t - t_0, & (3.16)\\ \frac{\mathrm{d}n}{\mathrm{d}t} &= -\mu n, & (3.17)\\ n(t_0, 0) &= \int_0^\infty b(a)n(t_0, a)\mathrm{d}a. & (3.18) \end{aligned}$$

so that

$$n(t,a) = n(t_0,0)\exp\left\{-\int_0^a \mu(\theta)\mathrm{d}\theta\right\} \tag{3.19}$$

$$= n(t-a,0)\exp\left\{-\int_0^a \mu(\theta)\mathrm{d}\theta\right\}. \tag{3.20}$$

We can write down an expression for $n(t-a,0)$ using Equation (3.6) together with Equations (3.14) and (3.20)

$$n(t,0) = \int_0^\infty b(a)n(t,a)\mathrm{d}a = \underbrace{\int_0^t b(a)n(t,a)\mathrm{d}a}_{(0<a<t)} + \underbrace{\int_t^\infty b(a)n(t,a)\mathrm{d}a}_{(t<a<\infty)}, \tag{3.21}$$

and, hence,

$$n(t,0) \equiv \int_0^t \left(b(a)n(t-a,0)\exp\left\{-\int_0^a \mu(\theta)\mathrm{d}\theta\right\}\right)\mathrm{d}a + \int_t^\infty \left(b(a)f(a-t)\exp\left\{-\int_{a-t}^a \mu(\theta)\mathrm{d}\theta\right\}\right)\mathrm{d}a. \tag{3.22}$$

Equation (3.22) defines $n(t,0)$ in terms of known functions and $n(\tau,0)$ (where $0 \le \tau < t$). Although this is a linear equation for $n(t,0)$, it is usually difficult to solve.

3.1.2 Worked Example

Consider a population with a constant death rate, $\mu(a) = \mu$, and a piecewise constant birth rate, $b(a) = bH(a_R - a)$. In more detail, suppose that $n(t,a)$ satisfies

$$\frac{\partial n}{\partial t} + \frac{\partial n}{\partial a} = -\mu n, \tag{3.23}$$

with $n(0,a) = 1$ and $n(t,0) = \int_0^\infty b(a)n(t,a)\mathrm{d}a$, where

$$b(a) = \begin{cases} b & \text{for } 0 < a < a_R, \\ 0 & \text{otherwise.} \end{cases} \tag{3.24}$$

As above, when constructing solutions for $n(t,a)$, we consider separately the regions for which $0 < t < a$ and $0 < a < t$.

Region 1. In this region $0 < t < a$ and so we have $\mu(a) = \mu$ and $f(a) = 1$ in Equation (3.14). It is straightforward to show that in this region

$$n(t,a) = e^{-\mu t}. \tag{3.25}$$

Region 2. In this region $0 < a < t$ and so Equations (3.20) and (3.22) supply

$$n(t,a) = n(t-a,0)e^{-\mu a} \qquad \text{where} \qquad n(t,0) = b\int_0^{a_R} n(t,a)\mathrm{d}a. \tag{3.26}$$

When solving Equation (3.26), we must consider separately the cases for which $0 < t < a_R$ and $a_R < t < \infty$.

Case 1. If $0 < t < a_R$, then

$$\begin{aligned} n(t,0) &= b\int_0^{a_R} n(t,a)\mathrm{d}a \\ &= b\int_0^{t} n(t,a)\mathrm{d}a + b\int_t^{a_R} n(t,a)\mathrm{d}a \\ &= b\int_0^{t} n(t-a,0)e^{-\mu a}\mathrm{d}a + b\int_t^{a_R} e^{-\mu t}\mathrm{d}a, \end{aligned} \tag{3.27}$$

where we have exploited the fact that $n(t,a) = e^{-\mu t}$ for $0 < t < a$. We rewrite Equation (3.27) in terms of $N(t) = n(t,0)$:

$$\begin{aligned} N(t) &= b\int_0^{t} N(t-a)e^{-\mu a}\mathrm{d}a + b(a_R - t)e^{-\mu t} \\ &= b\int_0^{t} N(\tau)e^{-\mu(t-\tau)}\mathrm{d}\tau + b(a_R - t)e^{-\mu t}. \end{aligned} \tag{3.28}$$

Differentiating this expression for $N(t)$ with respect to t we obtain the following ordinary differential equation for $N(t)$:

$$\frac{\mathrm{d}N}{\mathrm{d}t} = (b-\mu)N - be^{-\mu t}, \tag{3.29}$$

and hence we have

$$N(t) = \hat{N}e^{(b-\mu)t} + e^{-\mu t}, \tag{3.30}$$

where $\hat{N}$ is a constant of integration.

Substituting the expression for $N(t) = n(t,0)$ into Equation (3.26) and recalling that $n(t,a) = e^{-\mu t}$ for $0 < t < a$, we deduce that, for $0 < t < a_R$, our age-structured population evolves as follows:

$$n(t,a) = \begin{cases} N(t-a)e^{-\mu a} = e^{-\mu t}\left(\hat{N}e^{b(t-a)} + 1\right) & \text{for } 0 < a < t; \\ e^{-\mu t} & \text{for } 0 < t < a. \end{cases} \tag{3.31}$$

Case 2. For $a_R < t$, and with $N(t) = n(t,0)$, Equation (3.26) gives

$$N(t) = b\int_0^{a_R} N(t-a)e^{-\mu a}\mathrm{d}a = b\int_{t-a_R}^{t} N(\tau)e^{-\mu(t-\tau)}\mathrm{d}\tau. \tag{3.32}$$

If we differentiate this expression for $N(t)$ with respect to t we obtain a delay differential equation for $N(t)$:

$$\frac{\mathrm{d}N}{\mathrm{d}t} = (b-\mu)N(t) - bN(t-a_R)e^{-\mu a_R}. \tag{3.33}$$

We seek solutions of the form $N(t) = \tilde{N}e^{\omega t}$ where

$$\omega = (b-\mu) - be^{-(\omega+\mu)a_R}. \tag{3.34}$$

With $N(t) = \tilde{N}e^{\omega t}$, Equation (3.31) supplies

$$n(t,a) = N(t-a)e^{-\mu a} = \tilde{N}e^{\omega(t-a)}e^{-\mu a}. \tag{3.35}$$

If $\Re e(\omega) > 0$ then the age-dependent population increases over time; if $\Re e(\omega) < 0$ then it decays. For a stable, age-structured population, we require $\omega = 0$. From Equation (3.34) we deduce that the population will be stable if the birth rate b, the death rate μ and the parameter a_R satisfy

$$b = \frac{\mu}{1 - e^{-\mu a_R}}. \tag{3.36}$$

In this case where $\omega = 0$, we have

$$n(t,a) = \begin{cases} e^{-\mu a} & \text{for } 0 < a < t, \\ e^{-\mu t} & \text{for } a_R < t < a. \end{cases} \tag{3.37}$$

Notes and conclusions. Equation (3.36) states how the birth and death rates should be related in order to achieve a stable, age-structured population (*i.e.* one which neither explodes nor dies out). We can use this equation to draw the following conclusions:

- we must have $b > \mu$ – since only individuals of age $0 < a < a_R$ reproduce, the birth rate b must exceed the death rate to achieve a stable population;
- if $a_R \to \infty$, then $b \to \mu$ – if all individuals reproduce, then a stable population will only be achieved if the birth and death rates balance;
- if $a_R \to 0$, then $b \to 1/a_R \gg 1$ – as the reproductive lifespan of the population decreases, their birth rate must increase in order to maintain a stable population.

3.1.3 Separable solutions for age-structured models

Guided by the solution for the worked example, we now seek separable solutions to von Foerster's equation of the form

$$n(t,a) = e^{\gamma t}F(a), \tag{3.38}$$

i.e. we assume that the age distribution is altered by a time-dependent factor which decays or grows depending on whether $\Re e(\gamma) < 0$ or $\Re e(\gamma) > 0$. Substituting this separable form into Equation (3.4) supplies the following ordinary differential equation for $F(a)$:

$$\frac{\mathrm{d}F}{\mathrm{d}a} = -\left(\mu(a) + \gamma\right) F \quad \Longrightarrow \quad F(a) = F(0)\exp\left\{-\gamma a - \int_0^a \mu(\theta)\mathrm{d}\theta\right\}. \tag{3.39}$$

Imposing the boundary conditions stated in Equation (3.5) we deduce

$$\begin{aligned} n(t,0) &= e^{\gamma t}F(0) \\ &= \int_0^\infty b(a)e^{\gamma t}F(a)\mathrm{d}a \\ &= e^{\gamma t}F(0)\int_0^\infty b(a)\exp\left\{-\gamma a - \int_0^a \mu(\theta)\mathrm{d}\theta\right\}\mathrm{d}a. \end{aligned} \tag{3.40}$$

Cancelling by the nonzero factor $e^{\gamma t}F(0)$, we deduce

$$1 = \int_0^\infty b(a)\exp\left\{-\gamma a - \int_0^a \mu(\theta)\mathrm{d}\theta\right\}\mathrm{d}a \;\equiv\; \Phi(\gamma). \tag{3.41}$$

Since $\Phi(\gamma)$ is a monotonic decreasing function of γ, we deduce that Equation (3.41) admits a unique solution for γ.

In general, a separable solution will not satisfy the initial conditions $n(0,a) = f(a)$. However, in the limit as $t \to \infty$, Equation (3.22) supplies

$$n(t,0) \sim \int_0^t b(a)n(t-a,0)\exp\left\{-\int_0^a \mu(\theta)\mathrm{d}\theta\right\}\mathrm{d}a. \tag{3.42}$$

If we seek solutions to this equation of the form $n(t,a) \sim e^{\gamma t}F(a)$, then Equation (3.41) is recovered.

Exercise. By seeking separable solutions to the worked example, verify that Equation (3.41) is a necessary condition for obtaining a stable, age-structured population.

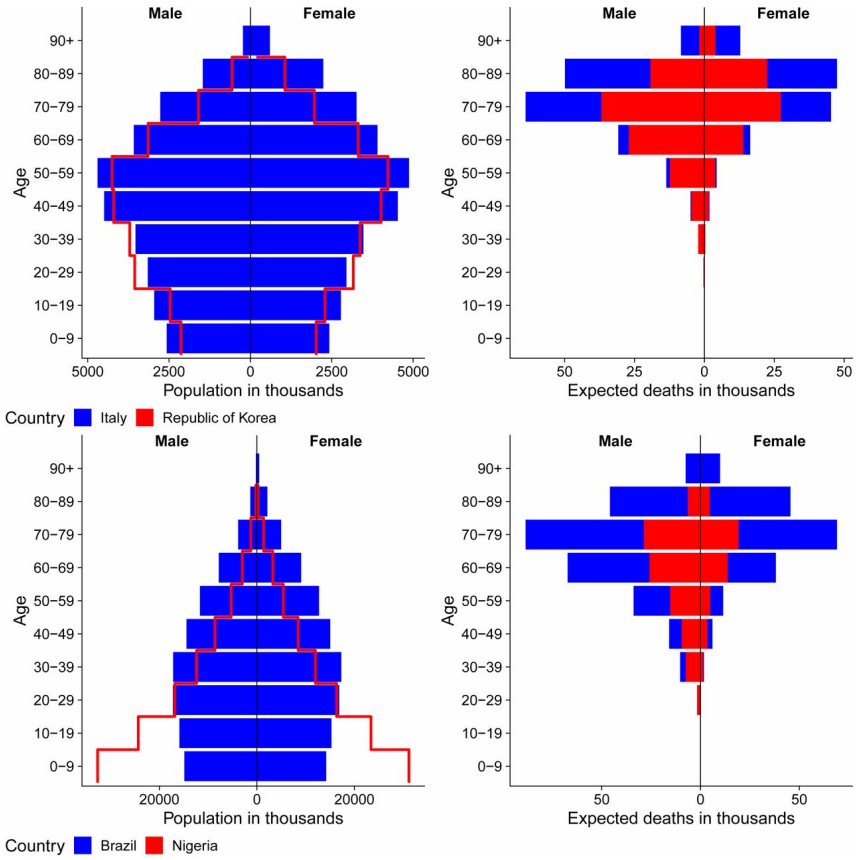

Figure 3.3: Population composition (left) and expected deaths in population (right) for Italy and Republic of Korea (top) and Nigeria and Brazil (bottom). Projections assume 10% population infection rate and age-sex-specific case fatality rates from Italy. Imaged reproduced from [1].

Exercise. Suppose that $\mu(a) = \mu$, constant, $n(0, a) = 1$ and $b(a)$ is given by

$$b(a) = \begin{cases} b, & \text{for } a_L < a < a_R, \\ 0, & \text{otherwise.} \end{cases} \tag{3.43}$$

By seeking separable solutions to von Foerster's equation, show that

$$b = \mu/(e^{-\mu a_L} - e^{-\mu a_R}), \tag{3.44}$$

is a necessary condition for obtaining a stable, age-structured population. Explain what happens in the limit at $(a_R - a_L) \to 0$.

3.2 Age-dependent epidemic models

One of the main reasons for developing age-structured models is to study the spread of diseases for which age is an important factor for susceptibility, infectiousness or death. For example, vulnerability to COVID increases dramatically with age (see Figure 3.3). In this section, we

will extend our previous age-structured model of population growth to describe the spread of a disease. In order to do this, we divide the population into two age-structured sub-populations: Susceptibles, $S(t,a)$, and Infectives, $I(t,a)$.

Applying the arguments used to derive Equation (3.4), we assume that $S(t,a)$ and $I(t,a)$ satisfy

$$\frac{\partial S}{\partial t}+\frac{\partial S}{\partial a} = -\underbrace{\left(\int_0^\infty r(\alpha)I(t,\alpha)\mathrm{d}\alpha\right)S(t,a)}_{\text{infection}}-\underbrace{\mu S}_{\text{death}}, \tag{3.45}$$

$$\frac{\partial I}{\partial t}+\frac{\partial I}{\partial a} = \underbrace{\left(\int_0^\infty r(\alpha)I(t,\alpha)\mathrm{d}\alpha\right)S(t,a)}_{\text{infection}}-\underbrace{\mu I}_{\text{death}}, \tag{3.46}$$

where, for simplicity, we assume that susceptibles and infectives die at the same, constant rate μ.

We close Equations (3.45)–(3.46) by prescribing the following initial and boundary conditions

$$S(0,a)=S_0(a), \qquad I(0,a)=I_0(a), \qquad S(t,0)=\int_0^\infty b(a)S(t,a)\mathrm{d}a, \qquad I(t,0)=0, \tag{3.47}$$

where the last condition results from the assumption that all newborns are susceptible.

In general, solutions for $S(t,a)$ and $I(t,a)$ require numerical approaches. Here, however, we attempt to make progress by seeking separable solutions of the form

$$S(t,a)=e^{\gamma t}S(a), \quad I(t,a)=e^{\gamma t}I(a), \tag{3.48}$$

with $\gamma=0$, *i.e.* we seek time-independent solutions. Then Equations (3.45)–(3.46) supply

$$\frac{\mathrm{d}S}{\mathrm{d}a} = -\left(\int_0^\infty r(\alpha)I(\alpha)\mathrm{d}\alpha\right)S(a)-\mu S, \tag{3.49}$$

$$\frac{\mathrm{d}I}{\mathrm{d}a} = \left(\int_0^\infty r(\alpha)I(\alpha)\mathrm{d}\alpha\right)S(a)-\mu I, \tag{3.50}$$

and hence

$$\frac{\mathrm{d}}{\mathrm{d}a}(S+I)=-\mu(S+I) \quad \Longrightarrow \quad S+I=\Lambda e^{-\mu a}, \tag{3.51}$$

where Λ is a constant of integration.

If $r(a)=r$, constant, then

$$\frac{\mathrm{d}I}{\mathrm{d}a}=r\underbrace{\left(\int_0^\infty I(\alpha)\mathrm{d}\alpha\right)}_{I_{\text{tot}}}S(a)-\mu I=rI_{\text{tot}}\Lambda e^{-\mu a}-\left(\mu+rI_{\text{tot}}\right)I, \tag{3.52}$$

which can be integrated to give

$$I(a) = Ae^{-(\mu+rI_{\text{tot}})a} + \Lambda e^{-\mu a}, \tag{3.53}$$

where

$$I_{\text{tot}} = \int_0^\infty I(a)\mathrm{d}a = \frac{A}{\mu + rI_{\text{tot}}} + \frac{\Lambda}{\mu}. \tag{3.54}$$

As a result,

$$I(a) = \left(I_{\text{tot}} - \frac{\Lambda}{\mu}\right)(\mu + rI_{\text{tot}})\, e^{-(\mu+rI_{\text{tot}})a} + \Lambda e^{-\mu a}. \tag{3.55}$$

and

$$S(a) = \Lambda e^{-\mu a} - I(a) = \left(\frac{\Lambda}{\mu} - I_{\text{tot}}\right)(\mu + rI_{\text{tot}})\, e^{-(\mu+rI_{\text{tot}})a} \tag{3.56}$$

where $S(0) = \int_0^\infty b(a)S(a)\mathrm{d}a$. Substituting for $S(0)$ and $S(a)$ we deduce that I_{tot} satisfies

$$1 = \int_0^\infty b(a)e^{-(\mu+rI_{\text{tot}})}\mathrm{d}a. \tag{3.57}$$

If $b(a) = b^{-\theta a}$, *i.e.* an individual's birth rate decreases with age, then

$$I_{\text{tot}} = \frac{b - \mu - \theta}{r}. \tag{3.58}$$

Exercise. Derive an expression for I_{tot} when $b(a) = bae^{-\theta a}$.

3.3 Structured models for populations of proliferating cells

Cells reproduce by duplicating their contents and then dividing in two (see Figure 3.4). The duration of the cell cycle varies widely: from eight minutes in fly embryos to more than a year for mammalian liver cells. In this subsection we will adapt the age-structured models developed above to study cell cycle dynamics.

We suppose that a tissue contains two types of cells:

- $p(t, s)$ = number of cycling cells at position $0 \leq s < T$ of the cell cycle at time t;
- $q(t, s)$ = number of quiescent (or non-cycling) cells arrested at position $0 \leq s < t$ at time t.

The evolution of the cycling population is governed by a nonlinear partial differential equation similar to Equation (3.4); as quiescent cells do not progress around the cell cycle, their evolution

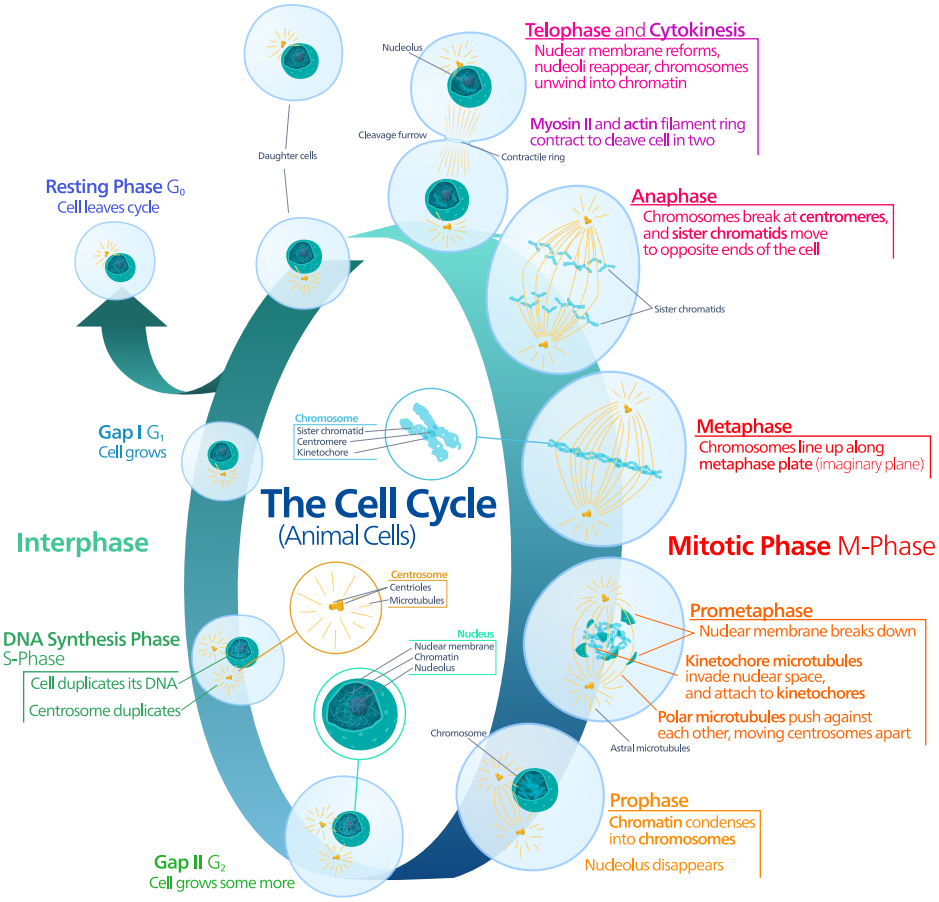

Figure 3.4: Schematic showing the different phases of the cycle cycle [16].

is governed by a time-dependent ordinary differential equation. In particular,

$$\frac{\partial p}{\partial t} + \frac{\partial p}{\partial s} = -\underbrace{\mu N p}_{\text{cell death}} - \underbrace{\Lambda N p}_{\text{exit cell cycle}} + \underbrace{\frac{\gamma q}{N_0 + N}}_{\text{re-enter cell cycle}}, \tag{3.59}$$

$$\frac{\partial q}{\partial t} = -\mu N q + \Lambda N p - \frac{\gamma q}{N_0 + N}. \tag{3.60}$$

where

$$N(t) = \int_0^T (p(t,s) + q(t,s))\mathrm{d}s, \tag{3.61}$$

is the total number of cells at time t, and μ, λ, γ and N_0 are positive constants.

In addition, we impose the following boundary and initial conditions:

$$p(0,s) = p_0(s), \qquad q(0,s) = q_0(s), \qquad p(t,0) = 2p(t,T). \tag{3.62}$$

The final condition states that at the end of the cell cycle (when $s = T$) a dividing cell produces two cells of age $s = 0$.

We seek separable solutions of the form

$$p(t,s) = e^{\theta t}P(s) \quad \text{and} \quad q(t,s) = e^{\theta t}Q(s), \tag{3.63}$$

with $\theta = 0$. Then $N(t)$, the total number of cells, is constant, and

$$\frac{\mathrm{d}P}{\mathrm{d}s} = -(\mu+\lambda)NP + \frac{\gamma Q}{N_0+N}, \tag{3.64}$$

$$0 = \Lambda NP - \left(\mu N + \frac{\gamma}{N_0+N}\right)Q, \tag{3.65}$$

hence

$$\frac{\mathrm{d}P}{\mathrm{d}s} = -\mu N(P+Q), \tag{3.66}$$

$$Q = \left(\frac{\Lambda N(N_0+N)}{\gamma+\mu N(N_0+N)}\right)P. \tag{3.67}$$

Eliminating Q we deduce

$$\frac{1}{P}\frac{\mathrm{d}P}{\mathrm{d}s} = -\mu N\left(1+\frac{\Lambda N(N_0+N)}{\gamma+\mu N(N_0+N)}\right) \equiv -\omega, \text{ say,} \tag{3.68}$$

and therefore

$$P(s) = P_\infty e^{-\omega s}, \tag{3.69}$$

$$Q(s) = Q_\infty e^{-\omega s} = \left(\frac{\Lambda N(N_0+N)}{\gamma+\mu N(N_0+N)}\right)P_\infty e^{-\omega s}. \tag{3.70}$$

Now using the fact that $P(s=0) = 2P(s=T)$ gives

$$1 = 2e^{-\omega T}, \tag{3.71}$$

and so

$$\frac{\ln 2}{T} = \omega = \mu N\left(1+\frac{\Lambda N(N_0+N)}{\gamma+\mu N(N_0+N)}\right). \tag{3.72}$$

This equation defines the total population size, N, in terms of the cell cycle length, T, and other model parameters.

We determine the proportion of cycling cells by noting that

$$N = \int_0^T [P(s)+Q(s)]\,\mathrm{d}s = \left(\frac{1-e^{-\omega T}}{\omega}\right)(P_\infty + Q_\infty), \tag{3.73}$$

which gives

$$2\omega N = \frac{\omega}{\mu N} P_\infty \quad \text{or} \quad P_\infty = 2\mu N^2, \tag{3.74}$$

and therefore

$$P(s) = 2\mu N^2 e^{-\omega s} \tag{3.75}$$

$$Q(s) = 2\mu N^2 \left(\frac{\Lambda N(N_0 + N)}{\gamma + \mu N(N_0 + N)} \right) e^{-\omega s}. \tag{3.76}$$

Exercise.

- Suppose $\gamma \to 0$: how are N, P and Q defined? Interpret your results.
- Suppose $\Lambda \to 0$: how are N, P and Q defined? Interpret your results.

Suggested reading.

- J. D. Murray, *Mathematical Biology, Volume I* – Chapter 1.
- A. G. McKendrick (1926). Applications of mathematics to medical problems. *Proc. Edinb. Math. Soc.* 44: 98-130. `https://doi.org/10.1017/S0013091500034428`
- F. Hoppensteadt, *Mathematical Theories of Populations: Demographics, Genetics and Epidemics,* (SIAM, 1975).

Chapter 4

Introduction to spatial variation

Both in the Part A *Mathematical Modelling in Biology* course, and this course so far, we have considered biological, biochemical and ecological phenomena for which spatial effects are not important. This is, however, often not the case. Consider a biochemical reaction as an example. Suppose this reaction involves solutes in a relatively large, *unstirred* solution. Then the system dynamics are governed not only by the rates at which the biochemicals react, but also by possible spatial variation in solute concentrations; in such cases, diffusion of the reactants can occur. Modelling such systems requires that we account for both reaction and diffusion.

A similar problem arises in population and ecological models when we wish to describe the tendency of a species to spread into a region it has not previously populated. Notable examples include ecological invasions, where one species invades another's territory (as with grey and red squirrels in the UK [11]), or the spread of disease. When developing mathematical descriptions of some, though by no means all, of these ecological and disease-spread systems, the appropriate transport mechanism is again diffusion; when modelling such systems we must include both reaction and diffusion. In addition, motile cells can move in response to external influences, such as chemical concentrations, light, mechanical stress and electric fields, among others. Of particular interest is modelling when motile cells respond to gradients in chemical concentrations, a process known as *chemotaxis*; we will also consider this scenario.

In the following chapters, we will learn how to model such phenomena and how (when possible) to solve and / or analyse the resulting partial differential equations, for a range of models drawn from biology, biochemistry and ecology. Most of the partial differential equations that we will

study can be written in the general form

$$\begin{pmatrix} \text{rate of change} \\ \text{of species} \end{pmatrix} = \begin{pmatrix} \text{net movement/flux} \\ \text{of species} \end{pmatrix} + \begin{pmatrix} \text{net rate of production} \\ \text{of species} \end{pmatrix}. \tag{4.1}$$

This is the **Principle of Mass Balance**.

4.1 Derivation of the reaction-diffusion equations

Let $i \in \{1, \ldots, m\}$. Suppose the chemical species C_i, of concentration c_i, is undergoing a reaction such that, in the absence of diffusion, one has

$$\frac{\mathrm{d}c_i}{\mathrm{d}t} = R_i(c_1, c_2, \ldots, c_m). \tag{4.2}$$

In Equation (4.2), $R_i(c_1, c_2, \ldots, c_m)$ is the total rate of production/destruction of C_i *per unit volume*, *i.e.* it is the rate of change of the concentration c_i.

Let t denote time, and $\boldsymbol{x}$ denote the position vector of a point in space. We define

- $c(\boldsymbol{x}, t)$ to be the concentration of a chemical (typically measured in mol m^{-3}).
- $\boldsymbol{q}(\boldsymbol{x}, t)$ to be the flux of the same chemical (typically measured in mol m^{-2} s^{-1}).

Now the flux of a chemical is defined such that, for a given infinitesimal surface element, of area $\mathrm{d}S$ and unit normal $\hat{\mathbf{n}}$, the amount of chemical flowing through the surface element in an infinitesimal time interval, of duration $\mathrm{d}t$, is given by

$$\hat{\mathbf{n}} \cdot \boldsymbol{q} \, \mathrm{d}S\mathrm{d}t. \tag{4.3}$$

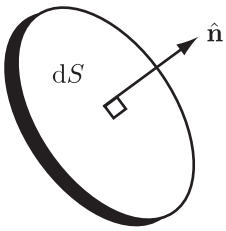

Definition. *Fick's Law of Diffusion* relates the flux $\boldsymbol{q}$ to the gradient of c via

$$\boldsymbol{q} = -D\nabla c, \tag{4.4}$$

where D, the diffusion coefficient, is independent of c and ∇c.

Using the Principle of Mass Balance, we have, for any closed volume V (fixed in time and space), with bounding surface ∂V,

$$\frac{\mathrm{d}}{\mathrm{d}t}\int_V c_i \, \mathrm{d}V = -\int_{\partial V} \boldsymbol{q} \cdot \mathbf{n} \, \mathrm{d}S + \int_V R_i(c_1, c_2, \ldots, c_m) \, \mathrm{d}V, \quad i \in \{1, \ldots, m\}. \tag{4.5}$$

Hence

$$\frac{\mathrm{d}}{\mathrm{d}t}\int_V c_i \,\mathrm{d}V = -\int_V \nabla\cdot\boldsymbol{q}\,\mathrm{d}V + \int_V R_i(c_1,c_2,\ldots,c_m)\,\mathrm{d}V \tag{4.6}$$

$$= \int_V \{\nabla\cdot(D_i\nabla c_i) + R_i(c_1,c_2,\ldots,c_m)\}\,\mathrm{d}V, \tag{4.7}$$

and thus for any closed volume, V, with surface ∂V, we have

$$\int_V \left\{\frac{\partial c_i}{\partial t} - \nabla\cdot(D_i\nabla c_i) - R_i\right\}\mathrm{d}V = 0, \quad i\in\{1,\ldots,m\}. \tag{4.8}$$

Hence

$$\frac{\partial c_i}{\partial t} = \nabla\cdot(D_i\nabla c_i) + R_i, \quad \boldsymbol{x}\in\mathcal{D}, \tag{4.9}$$

which constitutes a system of reaction-diffusion equations for the m chemical species in the finite domain $\mathcal{D}$. Such equations must be supplemented with initial and boundary conditions for each of the m chemicals.

Warning. Given, for example, that

$$\int_0^{2\pi}\cos\theta\,\mathrm{d}\theta = 0 \quad \not\Rightarrow \quad \cos\theta = 0, \quad \theta\in[0,2\pi], \tag{4.10}$$

are you sure one can deduce Equation (4.9)?

Suppose

$$\frac{\partial c_i}{\partial t} - \nabla\cdot(D_i\nabla c_i) - R_i \neq 0, \tag{4.11}$$

at some $\boldsymbol{x} = \boldsymbol{x}^*$. Without loss of generality, we can assume the above expression is positive *i.e.* the left-hand side of Equation (4.11) is positive. Then $\exists\,\epsilon > 0$ such that

$$\frac{\partial c_i}{\partial t} - \nabla\cdot(D_i\nabla c_i) - R_i > 0, \tag{4.12}$$

for all $\boldsymbol{x}\in\mathcal{B}_\epsilon(\boldsymbol{x}^*)$. In this case

$$\int_{\mathcal{B}_\epsilon(\boldsymbol{x}^*)}\left[\frac{\partial c_i}{\partial t} - \nabla\cdot(D_i\nabla c_i) - R_i\right]\mathrm{d}V > 0, \tag{4.13}$$

contradicting our original assumption, Equation (4.8). Hence our initial supposition is false and Equation (4.9) holds for $\boldsymbol{x}\in\mathcal{D}$.

Remark. With one species that has a constant diffusion coefficient, in the absence of reactions, we have the diffusion equation. In one spatial dimension this reduces to

$$\frac{\partial c}{\partial t} = D\frac{\partial^2 c}{\partial x^2}. \tag{4.14}$$

For a given length scale, L, and diffusion coefficient, D, the timescale of the system is $T = L^2/D$. For a cell, $L \sim 10^{-5}\text{m} = 10^{-3}\text{cm}$, and for a typical protein $D \sim 10^{-7}\text{cm}^2\text{s}^{-1}$ would not be unreasonable. Thus the timescale for diffusion to homogenise spatial gradients of a typical protein within a cell is

$$T \sim \frac{L^2}{D} \sim \frac{10^{-6}\ \text{cm}^2}{10^{-7}\ \text{cm}^2\ \text{s}^{-1}} \sim 10\ \text{s}, \tag{4.15}$$

therefore we can often neglect diffusion in a cell. However, as the length scale doubles, the time scale squares *e.g.* $L \mapsto L \times 10 \Rightarrow T \mapsto T \times 10^2$ and $L \mapsto L \times 10^2 \Rightarrow T \mapsto T \times 10^4$.

Note. The derivation of the reaction-diffusion equations generalises to situations other than modelling chemical or biochemical diffusion. For example, let $I(x, y, t)$ denote the number of infected people per unit area. Assume the infectives, on average, spread out via a random walk and interact with susceptibles, as described by the Law of Mass Action (see Section 5.2.1). Then the flux of infectives, $\boldsymbol{q}_I$, is given by

$$\boldsymbol{q}_I = -D_I \nabla I, \tag{4.16}$$

where D_I is a constant, with dimensions of (length)^2 (time)$^{-1}$. Thus, via precisely the same ideas and arguments as above, we have that

$$\frac{\partial I}{\partial t} = \nabla \cdot (D_I \nabla I) + rIS - aI, \tag{4.17}$$

where $S(x, y, t)$ is the number of susceptibles per unit area, and r is the rate at which susceptibles become infected on contact with infecteds, and a is the rate at which infecteds recover from the disease (see Section 5.2.1 for more details).

Fisher–KPP equation. A common example is the combination of logistic growth and diffusion which, in one spatial dimension, gives rise to the Fisher–KPP equation:

$$\frac{\partial u}{\partial t} = D\frac{\partial^2 u}{\partial x^2} + ru\left(1 - \frac{u}{K}\right). \tag{4.18}$$

This equation was first proposed to model the spread of an advantageous gene through a population. See Section 5.1 for more details.

4.2 Chemotaxis

As briefly mentioned earlier, motile cells can move in response to spatial gradients in chemical concentrations, a process known as chemotaxis. This leads to slightly more complicated transport equations, as we shall see [6].

The diffusive flux for the population density of the cells, n, is as previously: $\boldsymbol{J}_D = -D_n \nabla n$. The flux due to chemotaxis (assuming it is an attractant rather than a repellent) takes the form

$$\boldsymbol{J}_C = n\chi(c)\nabla c = n\nabla\Phi(c), \tag{4.19}$$

where c is the chemical concentration and $\Phi(c)$ increases monotonically with c. Clearly $\chi(c) = \Phi'(c)$; the cells move in response to a gradient of the chemical in the direction in which the function $\Phi(c)$ is increasing at the fastest rate. Thus the total flux $\boldsymbol{J}$ is

$$\boldsymbol{J} = \boldsymbol{J}_D + \boldsymbol{J}_C = -D_n \nabla n + n\chi(c)\nabla c. \tag{4.20}$$

If we assume that the behaviour of the cells is dominated by their diffusive and chemotactic transport together with their rate of reproduction and/or death, then we can use the Principle of Mass Balance to derive a partial differential equation that describes how their distribution changes over time. We need an additional reaction-diffusion partial differential equation for the evolution of chemical concentration. We assume it diffuses and, typically, is secreted and degrades. In this way, we arrive at the following equations for the cells, n, and the cell-derived chemical, c:

$$\frac{\partial n}{\partial t} = \nabla \cdot (D_n \nabla n) - \nabla \cdot (n\chi(c)\nabla c) + f(n, c); \tag{4.21}$$

$$\frac{\partial c}{\partial t} = \nabla \cdot (D_c \nabla c) + \lambda n - \mu c. \tag{4.22}$$

In the above the above $f(n, c)$ is often taken to be a logistic growth term while the function $\chi(c)$ describing chemotaxis has many forms, including

$$\chi(c) = \frac{\chi_0}{c}, \tag{4.23}$$

$$\chi(c) = \frac{\chi_0}{(k + c)^2}, \tag{4.24}$$

where the latter represents a receptor law, with $\Phi(c)$ taking a Michaelis-Menten form [6].

4.3 Positional information and pattern formation

Patterns are ubiquitous in biology. Consider, for example, animal coat markings on tigers, leopards and tropical fish. Consider, also, the well-defined pattern of bones and digits (fingers, thumbs and toes) and teeth that appear during human development. There are two main theories about how such patterns arise:

- Alan Turing's concept of **diffusion-driven instability** which we will study in Chapter 6. Turing's original paper was published in 1952 [14]);
- Lewis Wolpert's theory of **positional information** which is often also known as the French Flag Model (see [17]). We will study this theory below.

4.3.1 The French Flag Model

Consider a one-dimensional chain of cells that occupies the region $0 \leq x \leq L$. Suppose that a morphogen (signalling molecule), $m(x,t)$, enters the domain through $x = 0$, diffuses across the domain (with diffusion coefficient D), and is removed at $x = L$. If we assume that initially there is no morphogen in the domain, then the distribution of $m(x,t)$ can be described by the following equation

$$\frac{\partial m}{\partial t} = D\frac{\partial^2 m}{\partial x^2}, \tag{4.25}$$

with

$$m(0,t) = m_0, \quad m(L,t) = 0, \quad m(x,0) = 0, \tag{4.26}$$

where the positive constant m_0 defines the morphogen concentration at $x = 0$.

We assume that the morphogen rapidly establishes a fixed spatial profile, $m_s(x)$, which we determine by setting $\partial m/\partial t = 0$ in Equation (4.25):

$$\frac{\mathrm{d}^2 m_s}{\mathrm{d}x^2} = 0 \quad \Longrightarrow \quad m_s(x) = m_0\left(1 - \frac{x}{L}\right). \tag{4.27}$$

The French Flag Model then assumes that cells on the left (near $x = 0$) sense high morphogen levels and respond in some way (*e.g.* they turn blue), whilst cells in the centre and on the right sense intermediate and low levels of morphogen, respectively, and response in different ways (*e.g.* they turn white and red, respectively). See Figure 4.1 for an illustration.

To determine the widths of the red, white and blue regions, we introduce the positive constants

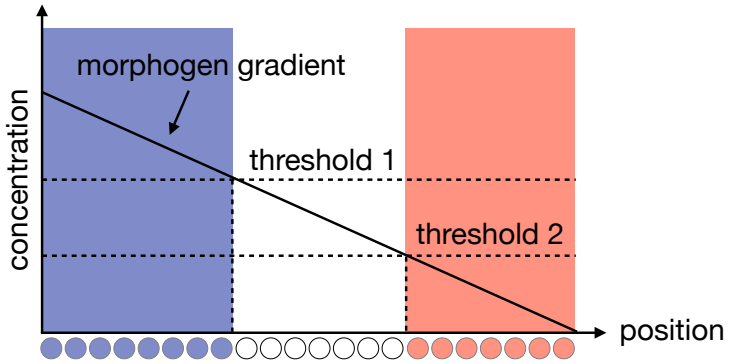

Figure 4.1: Schematic diagram of the French Flag Model. Cells that experience a morphogen concentration above threshold 1 turn blue, those that experience a morphogen concentration between threshold 1 and threshold 2 turn white, and those that experience a morphogen concentration below threshold 2 turn red.

$0 < m_W < m_B < m_0$ and define the spatial locations $0 < x_B < x_W < L$ such that

$$m_s(x = x_B) = m_B, \quad m_s(x = x_W) = m_W. \tag{4.28}$$

It is straightforward to show:

$$\text{width of blue region} = x_B = \left(1 - \frac{m_B}{m_0}\right) L; \tag{4.29}$$

$$\text{width of white region} = x_W - x_B = \left(\frac{m_B}{m_0} - \frac{m_W}{m_0}\right) L; \tag{4.30}$$

$$\text{width of red region} = L - x_W = \left(\frac{m_W}{m_0}\right) L. \tag{4.31}$$

Notes.

- The sizes of the red, white and blue regions are independent of the morphogen diffusion coefficient: do you think this is realistic?
- How do the widths of the different regions change as the domain size, L, and the right-hand boundary concentration, m_0, are varied? How do they depend on the threshold morphogen levels m_B and m_W?
- More complex models for positional information can be developed, to account for *e.g.* multiple morphogens, different boundary conditions and the decay of morphogens as they diffuse across the domain.
- In other biological applications (*e.g.* the intestinal crypt), positional information may determine whether cells proliferate, mature and/or die and, in this way, specify tissue size. In Chapter 6, we will study problems of this type, where the domain size depends on the distribution of a morphogen.

4.4 Minimum domains for spatial structure

Finally in this chapter, we explore whether there may be constraints on the size of a domain in terms of being able to support the growth of a population. To do so, we consider a dimensionless model for budworm dynamics. The budworm spread by diffusion on a one-dimensional domain, $0 \leq x \leq L$, and undergo logistic growth and predation by birds:

$$\frac{\partial u}{\partial t} = D\frac{\partial^2 u}{\partial x^2} + f(u), \quad \text{where} \quad f(u) = ru\left(1 - \frac{u}{q}\right) - \frac{u^2}{1+u^2}. \tag{4.32}$$

We suppose that exterior to the domain conditions are extremely hostile to budworm so that we have the boundary conditions

$$u(0,t) = 0, \quad u(L,t) = 0. \tag{4.33}$$

Clearly $u = 0$ is a solution of Equations (4.32)–(4.33). However, if we start with a small initial distribution of budworm, will the budworm die out, or will there be an outbreak of budworm? In particular, how does what happens depend on the domain size?

For initial conditions with $0 \leq u(x,0) \ll 1$, *i.e.* where there is initially a sufficiently small outbreak, we can approximate $f(u)$ by $f'(0)u = ru$, at least while $u(x,t)$ remains small. Then Equations (4.32)–(4.33) are, approximately,

$$\frac{\partial u}{\partial t} = D\frac{\partial^2 u}{\partial x^2} + f'(0)u, \quad \text{with} \quad u(0,t) = 0, \quad u(L,t) = 0. \tag{4.34}$$

We look for a solution of the form (invoking completeness of Fourier series)

$$u(x,t) = \sum_{n=1}^{\infty} a_n(t) \sin\left(\frac{n\pi x}{L}\right). \tag{4.35}$$

This gives that the time-dependent coefficients satisfy

$$\frac{\mathrm{d}a_n}{\mathrm{d}t} = -\frac{Dn^2\pi^2}{L^2}a_n + f'(0)a_n = \sigma_n a_n, \tag{4.36}$$

and hence

$$u(x,t) = \sum_{n=1}^{\infty} a_n(0) \exp\left[\left(f'(0) - \frac{Dn^2\pi^2}{L^2}\right)t\right] \sin\left(\frac{n\pi x}{L}\right). \tag{4.37}$$

For the solution to decay to zero, *i.e.* for the outbreak to die out, we require that all Fourier modes decay to zero as $t \to \infty$. Hence, we require that

$$\sigma_n < 0 \quad \forall n \quad \Longrightarrow \quad f'(0) - \frac{Dn^2\pi^2}{L^2} < 0 \quad \forall n, \tag{4.38}$$

or, equivalently,

$$f'(0) < \frac{Dn^2\pi^2}{L^2} \quad \Longrightarrow \quad L \leq \sqrt{\frac{D\pi^2}{f'(0)}} \stackrel{\text{def}}{=} L_{\text{crit}}. \tag{4.39}$$

Hence there is a critical lengthscale, L_{crit}, beyond which an outburst of budworm is possible in a spatially distributed system.

4.4.1 Domain size

On first inspection it is perhaps surprising that L_{crit} increases with the diffusion coefficient, *i.e.* diffusion is destabilising the zero steady state. We can further investigate how the nature of a steady state pattern depends on the diffusion coefficient.

Suppose $L > L_{\text{crit}}$, and we shift coordinates so that $x \in [-L/2, L/2]$ with

$$u(-L/2, t) = 0, \quad u(L/2, t) = 0, \tag{4.40}$$

and that the steady state is of the form shown in the right-hand figure.

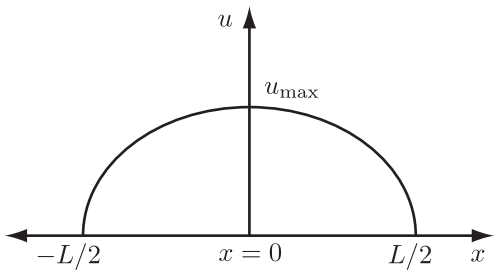

At steady state we have

$$0 = D\frac{\partial^2 u}{\partial x^2} + f(u). \tag{4.41}$$

Multiplying by $\partial u/\partial x$ and integrating with respect to x gives

$$0 = \int D\frac{\partial u}{\partial x}\frac{\partial^2 u}{\partial x^2}\,\mathrm{d}x + \int \frac{\partial u}{\partial x} f(u)\,\mathrm{d}x. \tag{4.42}$$

Thus we have

$$\frac{1}{2}D\left(\frac{\partial u}{\partial x}\right)^2 + F(u) = \text{constant} = F(u_{\max}) \quad \text{where} \quad F'(u) = f(u). \tag{4.43}$$

We can therefore find a relation between L, D, integrals of

$$F(u) \stackrel{\text{def}}{=} \int_0^u f(y)\,\mathrm{d}y, \tag{4.44}$$

and $u_{\max}$, the maximum size of the outbreak. From Equation (4.43) we have

$$\frac{\partial u}{\partial x} = -\left(\frac{2}{D}\right)^{\frac{1}{2}} \sqrt{F(u_{\max}) - F(u)}, \tag{4.45}$$

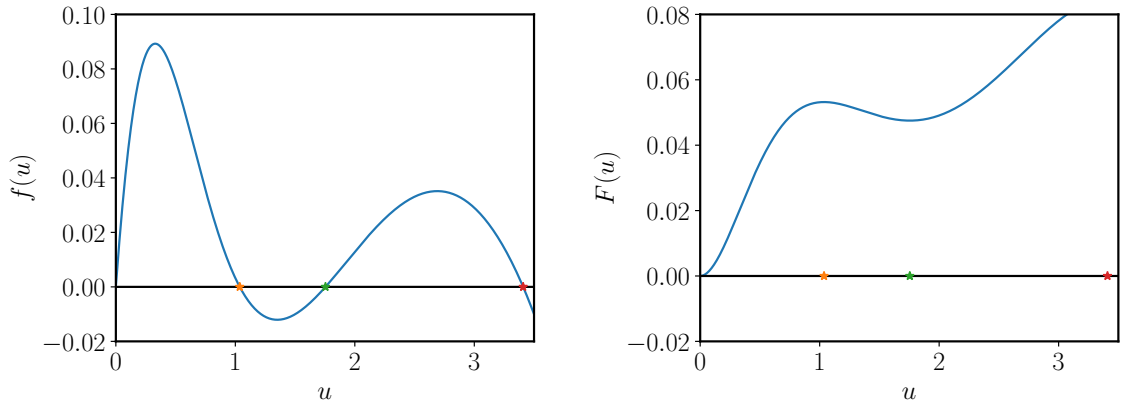

Figure 4.2: Plots of $f(u)$ and $F(u)$ with the three non-zero steady states indicated. Parameters are $r = 0.6$, $q = 6.2$ and $D = 0.1$.

since $x > 0$ and therefore $\partial u/\partial x < 0$. Plots of $f(u)$ and $F(u)$ are shown in Figure 4.2.

Integrating, gives

$$2\int_0^{L/2} \mathrm{d}x = -(2D)^{\frac{1}{2}} \int_{u_{\max}}^{0} \frac{1}{\sqrt{F(u_{\max}) - F(\bar{u})}}\,\mathrm{d}\bar{u}, \tag{4.46}$$

and hence

$$\frac{L}{\sqrt{2D}} = \int_0^{u_{\max}} \frac{1}{\sqrt{F(u_{\max}) - F(\bar{u})}}\,\mathrm{d}\bar{u}. \tag{4.47}$$

Therefore $u_{\max}$ is a function of $L/\sqrt{2D}$ and the root of Equation (4.47), as shown in Figure 4.3.

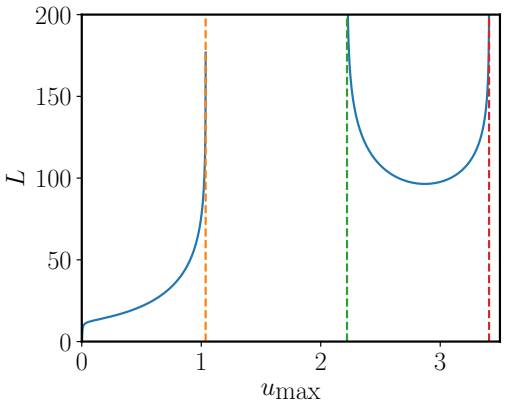

Figure 4.3: Numerical simulation of the $u_{\max}$-L space, given by Equation (4.47). Parameters are $r = 0.6$, $q = 6.2$ and $D = 0.1$.

Suggested reading.

- J. D. Murray, *Mathematical Biology, Volume I* – Chapter 11.
- N. F. Britton, *Essential Mathematical Biology* – Chapter 5.

Chapter 5

Travelling waves

Huge numbers of phenomena in biology exhibit wave phenomena, where a wave of *e.g.* chemical concentration, mechanical deformation or electrical signal propagates through a domain to effect a process. Examples include the spread of epidemics through susceptible populations, the healing of skin wounds, the invasion of insects and the waves of calcium concentration in early embryo development. In this chapter we will be interested in travelling waves, *i.e.* in waves that move at constant speed and without change in shape. We will learn how to analyse the models and draw useful conclusions about when we might see travelling waves, and how the speed of wave propagation and the shape of the wave depend on the model parameters.

The models we will study will be of reaction-diffusion type *e.g.*

$$\frac{\partial u}{\partial t} = D\frac{\partial^2 u}{\partial x^2} + f(u), \tag{5.1}$$

where D is the diffusion coefficient and $f(u)$ represents the reaction kinetics. In contrast to simple diffusion models of the form

$$\frac{\partial u}{\partial t} = D\frac{\partial^2 u}{\partial x^2}, \tag{5.2}$$

we will show that when both reaction and diffusion are present travelling waves can effect a change in system state very much faster than when diffusion alone governs the dynamics.

5.1 Fisher–KPP equation: a simple investigation

Fisher's equation, also known as the Kolmogorov–Petrovsky–Piskunov equation, or Fisher–KPP equation, is a simple, classical model that displays travelling waves. In one spatial dimension it

can be written as

$$\frac{\partial u}{\partial t} = D\frac{\partial^2 u}{\partial x^2} + ru\left(1 - \frac{u}{K}\right) \quad \text{for } x \in (-\infty, \infty) \text{ and } t > 0, \tag{5.3}$$

where $D > 0$ is the diffusion coefficient, $r > 0$ is the population growth rate and K is the population carrying capacity. The model was suggested by Fisher as a model for the spatial spread of a favoured gene through a population. But we can also think of it as the natural extension of the logistic model for population growth to the spatial setting, where the population disperses by diffusion. We will use the Fisher-KPP equation as a paradigm for the study of travelling wave behaviour more generally. All the steps that we will use to analyse the model are relevant in other travelling wave scenarios.

5.1.1 Non-dimensionalisation

First, we non-dimensionalise using the following scalings

$$\tilde{u} = \frac{u}{K}, \qquad \tilde{x} = x\sqrt{\frac{r}{D}}, \qquad \tilde{t} = rt. \tag{5.4}$$

Substituting the above scalings into Equation (5.3), and dropping the $\tilde{\text{s}}$ for notational convenience, gives

$$\frac{\partial u}{\partial t} = \frac{\partial^2 u}{\partial x^2} + u(1-u) \quad \text{for } x \in (-\infty, \infty) \text{ and } t > 0. \tag{5.5}$$

Clearly the solution of the Fisher–KPP equation will depend on the initial and boundary conditions we impose. For the time being, we will state these conditions as

$$u(x,t) \to u_{\pm\infty} \quad \text{as} \quad x \to \pm\infty \quad \text{and} \quad u(x,0) = u_0(x), \tag{5.6}$$

where $u_{\pm\infty}$ are constants.

5.1.2 Change to travelling wave coordinates

We will investigate whether a solution exists for Equation (5.5) which propagates without a change in shape and at a constant (but as yet unknown) speed, c. Such wave solutions are defined to be *travelling wave solutions*. Our investigation of the existence of a travelling wave solution will be substantially easier if we first transform to the moving coordinate frame $z = x - ct$ as, by the definition of a travelling wave, the wave profile will be independent of time in a frame moving at speed c.

We will make the change of variables $z = x - ct$ and $\tau = t$. Using the chain rule we have

$$\frac{\partial}{\partial t} = \frac{\partial \tau}{\partial t}\frac{\partial}{\partial \tau} + \frac{\partial z}{\partial t}\frac{\partial}{\partial z} \quad \text{and} \quad \frac{\partial}{\partial x} = \frac{\partial \tau}{\partial x}\frac{\partial}{\partial \tau} + \frac{\partial z}{\partial x}\frac{\partial}{\partial x}, \tag{5.7}$$

i.e.

$$\frac{\partial}{\partial t} \mapsto \frac{\partial}{\partial \tau} - c\frac{\partial}{\partial x} \quad \text{and} \quad \frac{\partial}{\partial x} \mapsto \frac{\partial}{\partial z}. \tag{5.8}$$

Letting $u(x,t) = \hat{u}(z,\tau)$, the transformed Fisher–KPP equation, Equation (5.5), then becomes

$$\frac{\partial \hat{u}}{\partial \tau} - c\frac{\partial \hat{u}}{\partial z} = \frac{\partial^2 \hat{u}}{\partial z^2} + \hat{u}(1-\hat{u}) \quad \text{for } z \in (-\infty, \infty) \text{ and } \tau > 0. \tag{5.9}$$

Further noting that we seek a solution that is *time independent* in the (z,τ) coordinate system, we seek solutions $\hat{u}(z,\tau) = U(z)$, so that, letting $'$ denote differentiation with respect to z, U satisfies the ordinary differential equation

$$U'' + cU' + U(1-U) = 0 \quad \text{for } z \in (-\infty, \infty). \tag{5.10}$$

We need to choose appropriate boundary conditions as $z \to \pm\infty$ for Equation (5.10). These are the same as the boundary conditions for the full partial differential equation, Equation (5.5), but re-written in terms of z:

$$U(z) \to u_{\pm\infty} \quad \text{as} \quad z \to \pm\infty, \tag{5.11}$$

where the constants $u_{\pm\infty}$ are identical to those specified in Equation (5.6).

For the non-dimensionalised version of the Fisher-KPP equation, Equation (5.5), we require that $u_{\pm\infty}$ only take the values zero or unity: integrating Equation (5.10) with respect to z from $-\infty$ to ∞ gives

$$\int_{-\infty}^{\infty} \left[U'' + cU' + U(1-U)\right] \mathrm{d}z = 0, \tag{5.12}$$

i.e.

$$\left[U' + cU\right]_{-\infty}^{\infty} + \int_{-\infty}^{\infty} U(1-U)\,\mathrm{d}z = 0. \tag{5.13}$$

If we want $U \to$ constant as $z \to \pm\infty$ and U, U' finite for $\forall z$ we must have either $U \to 0$ or $U \to 1$ as $z \to \infty$ and similarly for $z \to -\infty$. For the particular choice of $U(-\infty) = 1$ and $U(\infty)) = 0$, we anticipate $c > 0$.

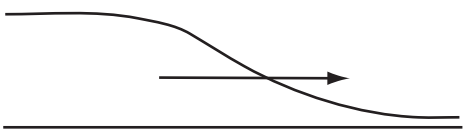

Indeed there are no solutions of the Fisher–KPP travelling wave equations with these boundary conditions and $c \leq 0$.

Notes.

- Solutions to Equations (5.5) and (5.6) are unique. The proof is an exercise in the theory of partial differential equations.
- The solutions of the travelling wave equation are not unique. One may have solutions for different values of the unknown c. Also, if $U(z)$ solves Equation (5.10) for any fixed value of c then, for the same value of c, so does $U(z + A)$, where A is any constant. For both c and A fixed the solution of the travelling wave equations are normally unique.
- Note that the solutions of the travelling wave equation, Equation (5.10), can only be solutions of the full partial differential equation, Equation (5.5), when considered on an infinite domain. Realistically one requires that the length scale of variation of the system in question is much less than the length scale of the physical domain for a travelling wave to (have the potential to) be an excellent approximation to the reaction-diffusion wave solutions on a physical, *i.e.* finite, domain.
- By seeking a travelling wave solution one "loses" the initial conditions associated with Equations (5.5) and (5.6). A solution of the travelling wave equation, Equation (5.10), is only a solution of the full partial differential equation, Equation (5.5), for all time if the travelling wave solution is consistent with the initial conditions specified in Equation (5.6). For a very large class of initial conditions, however, one finds instead that a solution of the full partial differential equation system, Equations (5.5) and (5.6), tends, as $t \to \infty$, to a solution of the travelling wave equation, Equation (5.10), with fixed c and A.
- The Russian mathematician Kolmogorov proved that, for a large class of initial conditions, solutions of the full partial differential equation system, Equations (5.5) and (5.6), tend, as $t \to \infty$, to a solution of the travelling wave equations with $c = 2$.

5.1.3 Phase plane analysis

We will first use phase plane analysis to investigate the nature of solutions of the Fisher–KPP equation, Equation (5.10), restated here for convenience,

$$U'' + cU' + U(1 - U) = 0 \quad \text{for } z \in (-\infty, \infty),$$

with the boundary conditions $U(-\infty) = 1$ and $U(\infty) = 0$ and $c > 0$.

To make progress we first transform to a system of first order ordinary differential equations by writing $U' = V$ to give

$$\frac{\mathrm{d}}{\mathrm{d}z}\begin{pmatrix} U \\ V \end{pmatrix} = \frac{\mathrm{d}}{\mathrm{d}z}\begin{pmatrix} U \\ U' \end{pmatrix} = \begin{pmatrix} V \\ -cV - U(1-U) \end{pmatrix} = \begin{pmatrix} f(U,V) \\ g(U,V) \end{pmatrix}. \tag{5.14}$$

This system has two steady states: at $(U,V) = (0,0)$ and $(U,V) = (1,0)$. To determine their linear stability, we linearise around the steady state, writing $U = U_s + \tilde{U}$ and $V = V_s + \tilde{V}$, where $\tilde{U}$ and $\tilde{V}$ are small perturbations and (U_s, V_s) the steady state, to write

$$\frac{\mathrm{d}}{\mathrm{d}z}\begin{pmatrix} \tilde{U} \\ \tilde{V} \end{pmatrix} = \boldsymbol{J}\begin{pmatrix} \tilde{U} \\ \tilde{V} \end{pmatrix}, \tag{5.15}$$

where $\boldsymbol{J}$ is the Jacobian matrix given by

$$\boldsymbol{J} = \left.\begin{pmatrix} \frac{\partial f}{\partial U} & \frac{\partial f}{\partial V} \\ \frac{\partial g}{\partial U} & \frac{\partial g}{\partial V} \end{pmatrix}\right|_{(U_s,V_s)} = \begin{pmatrix} 0 & 1 \\ -1 + 2U_s & -c \end{pmatrix}. \tag{5.16}$$

At $(0,0)$ we have

$$\det(\boldsymbol{J} - \lambda \boldsymbol{I}) = \det\begin{pmatrix} -\lambda & 1 \\ -1 & -c-\lambda \end{pmatrix} \quad \Longrightarrow \quad \lambda^2 + c\lambda + 1 = 0, \tag{5.17}$$

and hence

$$\lambda = \frac{-c \pm \sqrt{c^2 - 4}}{2}. \tag{5.18}$$

Therefore:

- if $c < 2$ we have $\lambda = -c/2 \pm i\mu$ and hence a stable spiral;
- if $c > 2$ we have $\lambda = -c/2 \pm \mu$ and hence a stable node;
- if $c = 2$ we have $\lambda = -1$ and hence a stable node.

At $(1,0)$ we have

$$\det(\boldsymbol{J} - \lambda \boldsymbol{I}) = \det\begin{pmatrix} -\lambda & 1 \\ 1 & -c-\lambda \end{pmatrix} \quad \Longrightarrow \quad \lambda^2 + c\lambda - 1 = 0, \tag{5.19}$$

and hence

$$\lambda = \frac{-c \pm \sqrt{c^2 + 4}}{2}. \tag{5.20}$$

Therefore $(1,0)$ is a saddle point.

Note 1. Solutions of the Fisher–KPP travelling wave equations must tend to phase plane stationary points as $z \to \pm\infty$. This is because $(U, V) = (U, U')$ will change as z increases, unless at a stationary point. Therefore they will keep moving along a phase space trajectory as $z \to \infty$ unless the $z \to \infty$ limit evolves to a stationary point. To satisfy $\lim_{z\to\infty} U(z) = 0$, we need to be on a phase space trajectory which "stops" at $U = 0$. Therefore we must be on a trajectory which tends to a stationary point with $U = 0$ as $z \to \infty$. Hence (U, U') must tend to $(0, 0)$ as $z \to \infty$ to satisfy $\lim_{z\to\infty} U(z) = 0$ as $z \to \infty$. An analogous argument holds as $z \to -\infty$.

Note 2. Solutions of Equation (5.10) with $c < 2$ are unphysical because if $c < 2$ then $U < 0$ at some point on the trajectory (close to the origin the solution looks like a spiral).

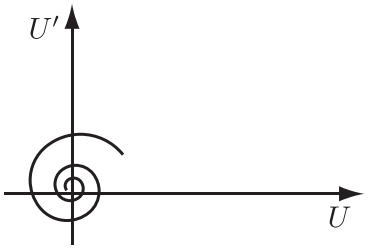

5.1.4 Existence and uniqueness

We will now investigate the existence and uniqueness of solutions of the Fisher–KPP equation, Equation (5.5), for $c \geq 2$ (so that we are considering only physically realistic travelling waves).

First, we consider the direction in which the trajectory leaving $(U, V) = (0, 1)$ travels. From Section 5.1.3 we know that the eigenvectors of the Jacobian, $\boldsymbol{J}$, at $(1, 0)$ satisfy

$$\begin{pmatrix} 0 & 1 \\ 1 & -c \end{pmatrix} \begin{pmatrix} 1 \\ q_\pm \end{pmatrix} = \lambda_\pm \begin{pmatrix} 1 \\ q_\pm \end{pmatrix} \quad \Longrightarrow \quad q_\pm = \lambda_\pm \quad \text{and} \quad 1 - cq_\pm = \lambda_\pm q_\pm. \tag{5.21}$$

Hence

$$\boldsymbol{v}_\pm = \begin{pmatrix} 1 \\ q_\pm \end{pmatrix} = \begin{pmatrix} 1 \\ \frac{1}{2}\left[-c \pm \sqrt{c^2+4}\right] \end{pmatrix}. \tag{5.22}$$

As a result, the gradient of the unstable manifold at $(U, V) = (1, 0)$ is given by

$$\frac{1}{2}\left(-c + \sqrt{c^2+4}\right) < \frac{1}{c}, \tag{5.23}$$

where the last inequality holds for $c \geq 2$ (this will be useful later for drawing the phase plane).

We can sketch the qualitative form of the phase plane trajectories near to the stationary point $(U, V) = (1, 0)$ for $c \geq 2$:

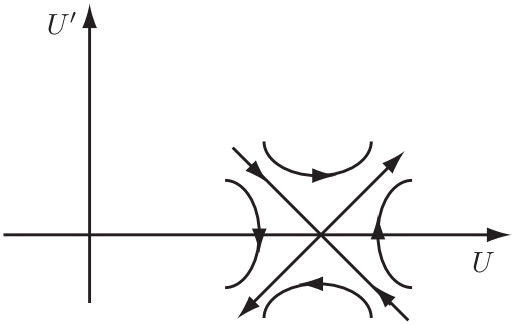

Close to the stationary point $(U, V) = (1, 0)$ we can then write

$$\begin{pmatrix} U \\ U \end{pmatrix} - \begin{pmatrix} U_s \\ V_s \end{pmatrix} = \begin{pmatrix} \tilde{U} \\ \tilde{V} \end{pmatrix} = a_- e^{\lambda_- z} \boldsymbol{v}_- + a_+ e^{\lambda_+ z} \boldsymbol{v}_+. \tag{5.24}$$

As a result, we see that any physically relevant phase plane trajectory must leave the saddle point $(U, V) = (1, 0)$ along the unstable manifold, which corresponds to a_+, in the direction of decreasing U.

We will now use a "trapping region" argument to demonstrate existence and uniqueness. This involves finding a region such that, for c fixed, the trajectory from the saddle point $(U, V) = (1, 0)$ enters the region, cannot leave, and is "funnelled" towards the stable node at $(U, V) = (0, 0)$.

For the trapping region we will take

$$\mathcal{R} \stackrel{\text{def}}{=} \{(U, V) \,:\, U \in [0, 1],\, V \leq 0,\, -V \leq U\}. \tag{5.25}$$

We begin by analysing the direction in which trajectories that cross the boundaries of $\mathcal{R}$ are moving: we want to establish that they all point into $\mathcal{R}$.

- Along $\mathcal{L}_1 = \{(U, V) \,:\, V = 0,\, U \in (0, 1)\}$ the trajectories point vertically into $\mathcal{R}$ as

$$\left|\frac{\mathrm{d}V}{\mathrm{d}U}\right| \to \infty \quad \text{as we approach } \mathcal{L}_1 \text{ and } cV' = -U(1-U) < 0. \tag{5.26}$$

- Along $\mathcal{L}_2 = \{(U, V) \,:\, U = 1,\, V \in (-1, 0)\}$ we have

$$\left.\frac{\mathrm{d}V}{\mathrm{d}U}\right|_{\mathcal{L}_2} = -c - \frac{U(1-U)}{V} = -c < 0, \tag{5.27}$$

  and so the trajectories point "diagonally upwards" into $\mathcal{R}$.

- Along $\mathcal{L}_3 = \{(U, V) \,:\, U \in [0, 1],\, V = -U\}$ we have

$$\left.\frac{\mathrm{d}V}{\mathrm{d}U}\right|_{\mathcal{L}_3} = -c + (1-U) = (-c+2) - (1+U) < -1, \tag{5.28}$$

  and so the trajectories also point "diagonally upwards" into $\mathcal{R}$.

Together, we have therefore shown that, for fixed $c \geq 2$, the single unstable manifold leaving $(U, V) = (1, 0)$ and entering the region $V < 0$, $U < 1$ enters, and can never leave, the region $\mathcal{R}$. Any trajectory must end at a stationary point, and trajectories are thus forced to the point $(U, V) = (0, 0)$.

As a result, we have shown that that, with $U \geq 0$ there is a solution to Equation 5.10 for every value of $c \geq 2$, and with $c \geq 2$ fixed, the phase space trajectory is unique. Moreover, the solution is monotonic as $V < 0$ throughout $\mathcal{R}$. Figure 5.1 shows the phase plane, with the null clines and travelling wave solution.

Note. For c fixed, the phase space trajectory of the Fisher–KPP travelling wave equation is unique. The non-uniqueness associated with the fact that if $U(z)$ solves the Fisher–KPP travelling wave equation then so does $U(z + A)$ for A constant simply corresponds to a shift along the phase space trajectory. This, in turn, corresponds to translation of the travelling wave.

Figure 5.1 shows the results of numerical simulation of the Fisher–KPP equation, Equation (5.5), with initial and boundary conditions given by Equation (5.6) at a series of time points.

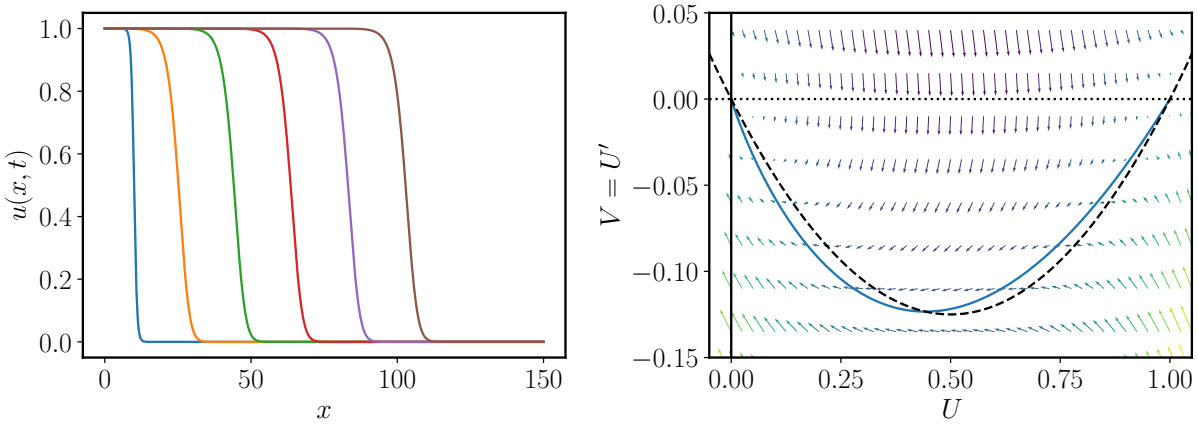

Figure 5.1: Left: Solution of the Fisher–KPP equation, Equation (5.5), with initial and boundary conditions given by Equation (5.6) at non-dimensional times $t = 0, 10, 20, 30, 40, 50$. Right: phase plane with the U null cline (dotted), V null cline (dashed) and the travelling wave solution (blue).

5.1.5 Relation between the travelling wave speed and initial conditions

We showed above that when the Fisher–KPP equation possesses a travelling wave solution then its wave speed satisfies $c^2 \geq 4$. When are such travelling wave solutions realised, and with what wave speeds? A rough estimate can be obtained by studying the Fisher–KPP equation near the leading front of the travelling wave where u is small. Linearising Equation (5.5) about $u = 0$ yields the following linear partial differential equation:

$$\frac{\partial u}{\partial t} = \frac{\partial^2 u}{\partial x^2} + u. \tag{5.29}$$

We will assume that

$$u(x, 0) \sim Be^{-ax} \quad \text{as } x \to \infty, \tag{5.30}$$

for $a, B > 0$ and seek travelling solutions of the linearised Fisher–KPP equation of the form

$$u(x,t) \sim Be^{-a(x-ct)}. \tag{5.31}$$

The linearised partial differential equation yields the following *dispersion relation* which defines the wave speed c in terms of the decay rate of the initial data

$$ac = a^2 + 1 \quad \Longrightarrow \quad c = a + \frac{1}{a} \geq 2, \tag{5.32}$$

with equality if and only if $a = 1$. We will consider separately the cases $a > 1$ and $a < 1$.

Case 1: $a < 1$**.** In this case

$$e^{-ax} > e^{-x}, \tag{5.33}$$

which implies that the initial conditions decay less rapidly than the travelling wave with minimum wave speed $c_{\min} = 2$. As a result, the behaviour is dominated by the initial conditions and $c = a + a^{-1}$.

Case 2: $a > 1$**.** In this case

$$e^{-ax} < e^{-x}, \tag{5.34}$$

which implies that the initial conditions decay more rapidly than the travelling wave with minimum wave speed $c_{\min} = 2$. As a result, the behaviour is dominated by the travelling wave with minimum wave speed $c_{\min} = 2$.

Non-Examinable: initial conditions of compact support

Kolmogorov considered the Fisher–KPP equation

$$\frac{\partial u}{\partial t} = \frac{\partial^2 u}{\partial x^2} + u(1-u) \quad \text{for } x \in (-\infty, \infty) \text{ and } t > 0,$$

with the boundary conditions

$$u(x,t) \to 1 \quad \text{as} \quad x \to -\infty \quad \text{and} \quad u(x,t) \to \quad \text{as} \quad x \to \infty, \tag{5.35}$$

and non-negative initial conditions such that there is an M, with $0 < M < \infty$, for which

$$u(x,0) = 0 \quad \text{for} \quad x > M \quad \text{and} \quad u(x,0) = 1 \quad \text{for} \quad x < -M. \tag{5.36}$$

He proved that $u(x,t)$ tends to a Fisher–KPP travelling wave solution with $c = 2$ as $t \to \infty$.

5.2 Models of epidemics

The study of infectious diseases has a long history and there are numerous detailed models of a variety of epidemics and epizootics (*i.e.* animal epidemics). Here we will only scratch the surface. In what follows we consider a basic model and show how it can be used to make general comments about epidemics and, in fact, approximately describe some specific epidemics.

5.2.1 The SIR model

Consider a disease for which the population can be placed into three compartments:

- the susceptible compartment, S, who can catch the disease;
- the infective compartment, I, who have and transmit the disease;
- the removed compartment, R, who have been isolated, or who have recovered and are immune to the disease, or have died due to the disease during the course of the epidemic.

We will make the following assumptions in order to build our model:

- the epidemic is of short duration course so that the population is constant (counting those who have died due to the disease during the course of the epidemic);
- the disease has a negligible incubation period;
- if a person contracts the disease and recovers, they are immune (and hence remain in the removed compartment);
- the numbers involved are sufficiently large to justify a continuum approximation, and there is sufficient population mixing to justify neglecting spatial effects;
- the dynamics of the disease can be described by applying the Law of Mass Action to the following "reactions"

$$S + I \xrightarrow{r} 2I, \quad \text{and} \quad I \xrightarrow{a} R. \tag{5.37}$$

Then the system of ordinary differential equations describing the time evolution of numbers in the susceptible, infective and removed compartments is

$$\frac{\mathrm{d}S}{\mathrm{d}t} = -rIS, \tag{5.38}$$

$$\frac{\mathrm{d}I}{\mathrm{d}t} = rIS - aI, \tag{5.39}$$

$$\frac{\mathrm{d}R}{\mathrm{d}t} = aI, \tag{5.40}$$

subject to

$$S(0) = S_0, \quad I(0) = I_0, \quad R(0) = 0. \tag{5.41}$$

Note that

$$\frac{\mathrm{d}}{\mathrm{d}t}(S + I + R) = 0 \quad \Longrightarrow \quad S + I + R = S_0 + I_0. \tag{5.42}$$

Key questions in an epidemic situation are, given r, a, S_0 and I_0,

1. Will the disease spread, *i.e.* will the number of infectives increase, at least in the short-term?
2. If the disease spreads, what will be the maximum number of infectives at any given time?
3. How many people in total catch the disease?

We can use simple analysis of the model equations to answer them.

First, we have

$$\frac{\mathrm{d}S}{\mathrm{d}t} = -rIS \quad \Longrightarrow \quad S \text{ is decreasing and therefore } S \leq S_0. \tag{5.43}$$

As a result,

$$\frac{\mathrm{d}I}{\mathrm{d}t} = I(rS - a) < I(rS_0 - a). \tag{5.44}$$

Therefore, if $S_0 < a/r$ the number of infectives never increases.

Second, we can write

$$\frac{\mathrm{d}I}{\mathrm{d}S} = -\frac{(rS - a)}{rS} = -1 + \frac{\rho}{S} \quad \text{where} \quad \rho \stackrel{\text{def}}{=} \frac{a}{r}. \tag{5.45}$$

Integrating gives

$$I + S - \rho \ln S = I_0 + S_0 - \rho \ln S_0, \tag{5.46}$$

and so, noting that $\mathrm{d}I/\mathrm{d}S = 0$ for $S = \rho$, the maximum number of infectives is given by

$$I_{\max} = \begin{cases} I_0 & S_0 \leq \rho \\ I_0 + S_0 - \rho \ln S_0 + \rho \ln \rho - \rho & S_0 > \rho \end{cases}. \tag{5.47}$$

Third, from Equations (5.43)-(5.44), $I \to 0$ as $t \to \infty$. Therefore the total number who catch the disease is

$$R(\infty) = N_0 - S(\infty) - I(\infty) = N_0 - S(\infty), \tag{5.48}$$

where $S(\infty) < S_0$ is the root of

$$S_\infty - \rho \ln S_\infty = N_0 - \rho \ln S_0, \tag{5.49}$$

obtained by setting $S = S_\infty$ and $N_0 = I_0 + S_0$ in Equation (5.46).

Figure 5.2 shows the phase plane with a number of trajectories marked.

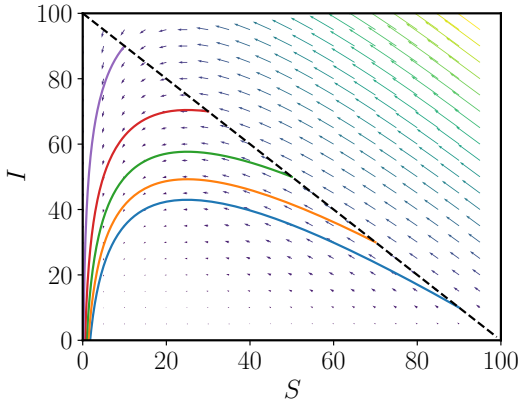

Figure 5.2: Phase space of the SIR model, Equations (5.38)–(5.40), where the solid lines indicate the phase trajectories and the dashed line is $S + I = S_0 + I_0$. Parameters are as follows: $r = 0.01$ and $a = 0.25$.

5.2.2 An SIR model with spatial heterogeneity

We now consider an application of the SIR modelling approach to the spread of fox rabies. We will make the same assumptions as for the standard SIR model (except the assumption that it is possible to neglect spatial effects), plus:

- healthy, *i.e.* susceptible, foxes are territorial and, on average, do not move from their territories;
- rabid, *i.e.* infective, foxes undergo behavioural changes and migrate randomly, with an effective, constant, diffusion coefficient D;
- rabies is fatal, so that infected foxes do not return to the susceptible compartment but die, and hence the removed compartment does not migrate.

Taking into account random motion of rabid foxes, the SIR equations become

$$\frac{\partial S}{\partial t} = -rIS, \tag{5.50}$$

$$\frac{\partial I}{\partial t} = D\nabla^2 I + rIS - aI, \tag{5.51}$$

$$\frac{\partial R}{\partial t} = aI. \tag{5.52}$$

The I and S equations decouple, and we consider these in more detail. We assume a one-dimensional spatial domain $x \in (-\infty, \infty)$, and non-dimensionalise the model using

$$\tilde{I} = \frac{I}{S_0}, \quad \tilde{S} = \frac{S}{S_0}, \quad \tilde{x} = \sqrt{\frac{rS_0}{D}}x, \quad \tilde{t} = rS_0 t \quad \text{and} \quad \lambda = \frac{a}{rS_0}, \tag{5.53}$$

where S_0 is the population density in the absence of rabies. The non-dimensionalised partial differential equations for I and S are then (after dropping the ˜s for notational convenience)

$$\frac{\partial S}{\partial t} = -IS, \tag{5.54}$$

$$\frac{\partial I}{\partial t} = \frac{\partial^2 I}{\partial x^2} + I(S - \lambda). \tag{5.55}$$

We will assume $\lambda = a/(rS_0) < 1$ below – this is equivalent to the condition for disease spread in the earlier SIR model.

Travelling wave analysis

We seek travelling wave solutions with $S(x,t) = S(z)$ and $I(x,t) = I(z)$ where $z = x - ct$ for $c > 0$. Letting $' = \mathrm{d}/\mathrm{d}z$ gives

$$0 = cS' - IS, \tag{5.56}$$

$$0 = I'' + cI' + I(S - \lambda). \tag{5.57}$$

As boundary conditions, we assume a healthy population as $z \to \infty$

$$S \to 1 \quad \text{and} \quad I \to 0, \tag{5.58}$$

and as $z \to -\infty$ we require

$$I \to 0. \tag{5.59}$$

Minimum wave speed. We can establish a lower bound on the travelling wave speed by writing $S = 1 - P$ and linearising about the wavefront:

$$-cP' - I = 0 \quad \text{and} \quad I'' + cI' + I(1 - \lambda). \tag{5.60}$$

The I equation decouples and analysis of this equation gives a stable focus at $(I, I') = (0, 0)$ if the eigenvalues

$$\mu = \frac{-c \pm \sqrt{c^2 - 4(1 - \lambda)}}{2}, \tag{5.61}$$

are real and negative. This requires

$$c \geq c_{\min} = 2\sqrt{1-\lambda}. \tag{5.62}$$

In typical situations the wave evolves to have minimum wave speed, $c_{\min}$.

Severity of the epidemic. The number of susceptible individuals left as $t \to \infty$, which is given by $S(-\infty)$ since in transforming to the travelling wave frame time is reversed, is a measure of the severity of the epidemic. We have $I = cS'/S$ and therefore

$$\frac{\mathrm{d}}{\mathrm{d}z}(I' + cI) + cS'\left(\frac{S-\lambda}{S}\right) = 0. \tag{5.63}$$

By integrating and evaluating Equation (5.63) as $z \to \infty$ we have

$$(I' + cI) + c(S - \lambda \ln S) = \text{constant} = c. \tag{5.64}$$

In this case the severity of the equation is given as the solution to

$$S(-\infty) - \lambda \ln S(-\infty) = 1, \quad \text{where} \quad S(-\infty) < 1. \tag{5.65}$$

Numerical results. Results from simulation of the full partial differential equation model are shown in Figure 5.3, and illustrate the formation of a travelling wave of infection through the susceptible population.

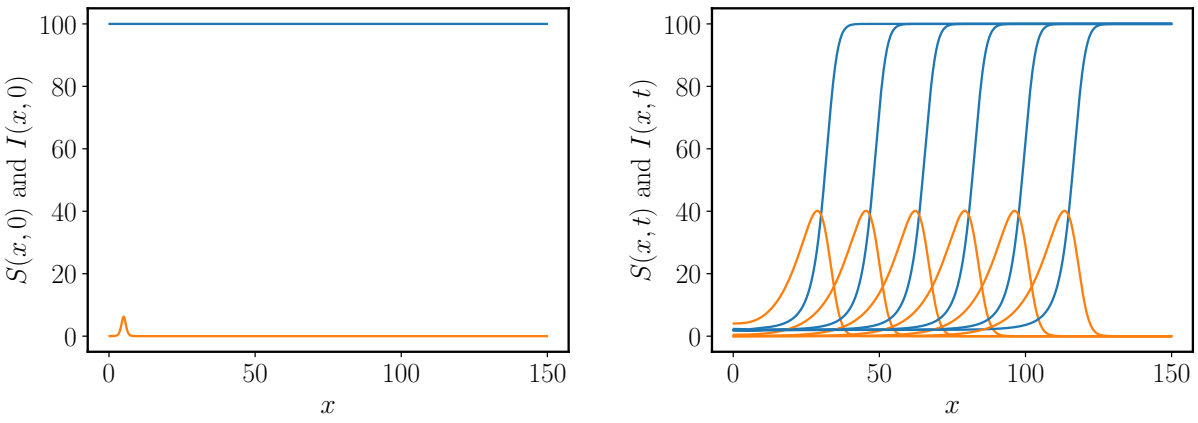

Figure 5.3: Solution of the fox rabies model, Equations (5.50)–(5.51), in one spatial dimension. Left: Initial conditions. Right: at times $t = 20, 30, 40, 50, 60, 70$. $S(x,t)$ is shown in blue and $I(x,t)$ in orange. Zero flux conditions are implemented at both boundaries. Parameters are as follows: $S_0 = 100$, $r = 0.01$ and $a = 0.25$.

Suggested reading.

- J. D. Murray, *Mathematical Biology, Volume I* – Chapter 13.
- J. D. Murray, *Mathematical Biology, Volume II* – Chapter 1.
- N. F. Britton, *Essential Mathematical Biology* – Chapter 5.

Chapter 6

Pattern formation

Examples of spatial pattern and structure can be seen just about everywhere in the natural world, and there are many outstanding questions about how these patterns are generated and maintained in a such robust and reproducible manner. We will focus attention on a class of reaction-diffusion models that generate patterns via what is known as a diffusion-driven instability. We will explore how to analyse the models to determine necessary conditions for a diffusion-driven instability, and how to predict the kinds of patterns that can form.

6.1 Diffusion-driven instability

We will consider a system that consists of two diffusible species, which diffuse and react according to the following coupled partial differential equations

$$\frac{\partial u}{\partial t} = D_u \nabla^2 u + f(u,v), \tag{6.1}$$

$$\frac{\partial v}{\partial t} = D_v \nabla^2 v + g(u,v), \tag{6.2}$$

for $\boldsymbol{x} \in \Omega$, $t \in [0,\infty)$ and Ω bounded. The initial conditions are

$$u(\boldsymbol{x},0) = u_0(\boldsymbol{x}), \quad v(\boldsymbol{x},0) = v_0(\boldsymbol{x}), \tag{6.3}$$

and the boundary conditions are either Dirichlet, *i.e.*

$$u = u_B, \quad v = v_B, \quad \boldsymbol{x} \in \partial\Omega, \tag{6.4}$$

or homogeneous Neumann, *i.e.*

$$\boldsymbol{n} \cdot \nabla u = 0, \quad \boldsymbol{n} \cdot \nabla v = 0, \quad \boldsymbol{x} \in \partial\Omega, \tag{6.5}$$

where $\boldsymbol{n}$ is the outward pointing normal on $\partial\Omega$.

We will be interested in analysing the pattern forming potential of this system where we define a pattern to be a stable, time-independent, spatially heterogeneous solution of Equations (6.1)–(6.2). In particular, we will be interested in patterns formed through a diffusion-driven instability.

Definition. A *diffusion-driven instability*, also referred to as a *Turing instability*, occurs when a spatially uniform steady state that is stable in the absence of diffusion becomes unstable when diffusion is present.

Note. Diffusion-driven instabilities can drive pattern formation in chemical systems and there is significant, but not necessarily conclusive, evidence that they can drive pattern formation in a variety of biological systems. A key point is that this mechanism can drive the system from close to a homogeneous steady state to a state with spatial pattern and structure. The fact that diffusion is responsible for this is initially quite surprising. Diffusion, in isolation, disperses a pattern; yet diffusion, combined with kinetic terms, can often drive a system towards a state with spatial structure.

6.1.1 Linear analysis

We wish to understand when a diffusion-driven instability occurs. We have

$$\frac{\partial}{\partial t}\begin{pmatrix} u \\ v \end{pmatrix} = \begin{pmatrix} D_u & 0 \\ 0 & D_v \end{pmatrix} \nabla^2 \begin{pmatrix} u \\ v \end{pmatrix} + \begin{pmatrix} f(u,v) \\ g(u,v) \end{pmatrix}, \tag{6.6}$$

for $\boldsymbol{x} \in \Omega$, $t \in [0, \infty)$, with

$$\boldsymbol{n}.\nabla u = 0 = \boldsymbol{n}.\nabla v, \quad \boldsymbol{x} \in \partial\Omega. \tag{6.7}$$

Using vector and matrix notation we define

$$\boldsymbol{u} = \begin{pmatrix} u \\ v \end{pmatrix}, \quad \boldsymbol{F}(\boldsymbol{u}) = \begin{pmatrix} f(u,v) \\ g(u,v) \end{pmatrix}, \quad \boldsymbol{D} = \begin{pmatrix} D_u & 0 \\ 0 & D_v \end{pmatrix}, \tag{6.8}$$

and write the problem with homogeneous Neumann boundary conditions as

$$\frac{\partial \boldsymbol{u}}{\partial t} = \boldsymbol{D}\nabla^2\boldsymbol{u} + \boldsymbol{F}(\boldsymbol{u}), \quad \boldsymbol{x} \in \Omega, \ t \in [0, \infty), \tag{6.9}$$

with

$$\boldsymbol{n} \cdot \nabla \boldsymbol{u} = 0, \quad \boldsymbol{x} \in \partial\Omega. \tag{6.10}$$

Let $\boldsymbol{u}_s$ be a steady state of the system *i.e.* such that $\boldsymbol{F}(\boldsymbol{u}_s) = \boldsymbol{0}$. Implicit in this definition is the assumption that $\boldsymbol{u}_s$ is a constant vector.

Let $\boldsymbol{w} = \boldsymbol{u} - \boldsymbol{u}_s$ with $|\boldsymbol{w}| \ll 1$. Then we have

$$\frac{\partial \boldsymbol{w}}{\partial t} = \boldsymbol{D}\nabla^2 \boldsymbol{w} + \boldsymbol{F}(\boldsymbol{u}_s) + \boldsymbol{J}\boldsymbol{w} + \text{higher order terms}, \tag{6.11}$$

where

$$\boldsymbol{J} = \left(\begin{array}{cc} \frac{\partial f}{\partial u} & \frac{\partial f}{\partial v} \\ \frac{\partial g}{\partial u} & \frac{\partial g}{\partial v} \end{array} \right) \Bigg|_{\boldsymbol{u}=\boldsymbol{u}_s}, \tag{6.12}$$

is the Jacobian of $\boldsymbol{F}$ evaluated at the spatially uniform steady state, $\boldsymbol{u} = \boldsymbol{u}_s$. Note that $\boldsymbol{J}$ is a *constant* matrix.

Neglecting higher order terms in $|\boldsymbol{w}|$, we have

$$\frac{\partial \boldsymbol{w}}{\partial t} = \boldsymbol{D}\nabla^2 \boldsymbol{w} + \boldsymbol{J}\boldsymbol{w}, \quad \boldsymbol{x} \in \Omega \quad \text{and} \quad \boldsymbol{n} \cdot \nabla \boldsymbol{w} = 0, \quad \boldsymbol{x} \in \partial\Omega. \tag{6.13}$$

This is a linear equation and so we look for a solution in the form of a linear sum of separable solutions. To do this, we must first consider a general separable solution given by

$$\boldsymbol{w}(\boldsymbol{x}, t) = A(t)\boldsymbol{p}(\boldsymbol{x}), \tag{6.14}$$

where $A(t)$ is a scalar function of time. Substituting from Equation (6.14) into Equation (6.13) yields

$$\frac{1}{A}\frac{\mathrm{d}A}{\mathrm{d}t}\,\boldsymbol{p} = \boldsymbol{D}\nabla^2 \boldsymbol{p} + \boldsymbol{J}\boldsymbol{p}. \tag{6.15}$$

Clearly to proceed, with $\boldsymbol{p}$ dependent on $\boldsymbol{x}$ only, we require $\dot{A}/A$ to be time independent. It must also be independent of $\boldsymbol{x}$ as A is a function of time only. Thus $\dot{A}/A$ is constant.

We take $\dot{A} = \lambda A$, where λ is an, as yet, undetermined constant. Thus

$$A = A_0 \exp(\lambda t), \tag{6.16}$$

for $A_0 \neq 0$ constant. Hence we require that our separable solution is such that

$$\lambda \boldsymbol{p} - \boldsymbol{J}\boldsymbol{p} - \boldsymbol{D}\nabla^2 \boldsymbol{p} = 0. \tag{6.17}$$

Suppose $\boldsymbol{p}$ satisfies the equation

$$\nabla^2 \boldsymbol{p} + k^2 \boldsymbol{p} = 0, \quad \boldsymbol{x} \in \Omega \quad \text{and} \quad \boldsymbol{n} \cdot \nabla \boldsymbol{p} = 0, \quad \boldsymbol{x} \in \partial\Omega, \tag{6.18}$$

where $k \in \mathbb{R}$. This is motivated by the fact that in one dimension on a bounded domain, we have $p'' + k^2 p = 0$; the solutions are trigonometric functions which means one immediately has a Fourier series when writing the sum of separable solutions.

Then we have

$$\left[\lambda \boldsymbol{I} - \boldsymbol{J} + \boldsymbol{D}k^2\right] \boldsymbol{p} = 0, \tag{6.19}$$

with $|\boldsymbol{p}|$ not identically zero. Hence, for a solution to exist we must have

$$\det\left[\lambda \boldsymbol{I} - \boldsymbol{J} + k^2 \boldsymbol{D}\right] = 0. \tag{6.20}$$

This can be rewritten as

$$\det \begin{pmatrix} \lambda - f_u + D_u k^2 & -f_v \\ -g_u & \lambda - g_v + D_v k^2 \end{pmatrix} = 0, \tag{6.21}$$

where the partial derivatives are evaluated at the spatially uniform steady state, $\boldsymbol{u}_s$. Expanding gives the following quadratic in λ

$$\lambda^2 + \left[(D_u + D_v)k^2 - (f_u + g_v)\right] \lambda + h(k^2) = 0, \tag{6.22}$$

where

$$h(k^2) = D_u D_v k^4 - (D_v f_u + D_u g_v)k^2 + (f_u g_v - g_u f_v). \tag{6.23}$$

Note 1. Fixing model parameters and functions (*i.e.* fixing D_u, D_v, f, g), we have an equation which gives λ as a function of k^2.

Note 2. For any k^2 such that Equation (6.18) possesses a solution, denoted $\boldsymbol{p}_k(\boldsymbol{x})$ below, we can find a $\lambda = \lambda(k^2)$ and, hence, a general separable solution of the form

$$A_0 e^{\lambda(k^2)t} \boldsymbol{p}_k(\boldsymbol{x}). \tag{6.24}$$

The most general solution formed by the sum of separable solutions is therefore

$$\sum_{k^2} A_0(k^2) e^{\lambda(k^2)t} \boldsymbol{p}_k(\boldsymbol{x}), \tag{6.25}$$

if there are countable k^2 for which Equation (6.18) possesses a solution. Otherwise the general solution formed by the sum of separable solutions is of the form

$$\int A_0(k^2)e^{\lambda(k^2)t}\boldsymbol{p}_{k^2}(\boldsymbol{x})\,\mathrm{d}k^2, \tag{6.26}$$

where k^2 is the integration variable.

Unstable points

If, for any k^2 such that Equation (6.18) possesses a solution, we find $\Re e(\lambda(k^2)) > 0$ then:

- $\boldsymbol{u}_s$ is (linearly) unstable and perturbations from the stationary state will grow;
- while the perturbations are small, the linear analysis remains valid. The perturbations grow until the linear analysis is invalid and the full non-linear dynamics comes into play;
- a small perturbation from the steady state develops into a growing spatially heterogeneous solution, which subsequently seeds spatially heterogeneous behaviour of the full non-linear model;
- a spatially heterogeneous pattern can emerge from the system from a starting point which is homogeneous to a very good approximation.

Stable points

If, for all k^2 such that Equation (6.18) possesses a solution, we find $\Re e(\lambda(k^2)) < 0$ then:

- $\boldsymbol{u}_s$ is (linearly) stable and perturbations from the stationary state do not grow;
- patterning will not emerge from perturbing the homogeneous steady state solution $\boldsymbol{u}_s$;
- the solution will decay back to the homogeneous solution.

Note. Strictly, this conclusion requires completeness of the separable solutions. This can be readily shown in one dimension on bounded domains (solutions of $p'' + k^2 p = 0$ on bounded domains with Neumann conditions are trigonometric functions and completeness is inherited from the completeness of Fourier series). Even if completeness of the separable solutions is not clear, numerical simulations of the full equations are highly indicative and do not, for the models typically encountered, contradict the results of the linear analysis. With enough effort and neglecting any biological constraints on model parameters and functions, one may well be able to find $D_u,\ D_v,\ f,\ g$ where there is such a discrepancy, but that is not the point of biological modelling.

6.2 Detailed study of the conditions for a Turing instability

For a Turing instability we require the homogeneous steady state to be **stable without diffusion** and **unstable with diffusion**. Here we analyse the requirements for each of these conditions to be satisfied. Note that, in the following analysis, all partial derivatives f_u, f_v, g_u and g_v are evaluated at the steady state, $\boldsymbol{u}_s$.

6.2.1 Stability without diffusion

First, we require that in the absence of diffusion the system is stable. This is equivalent to

$$\Re e(\lambda(0)) < 0, \tag{6.27}$$

for *all* solutions of $\lambda(0)$, as setting $k^2 = 0$ removes the diffusion terms in Equation (6.20) and the preceding equations.

We have that $\lambda(0)$ satisfies

$$\lambda(0)^2 - [f_u + g_v]\,\lambda(0) + [f_u g_v - f_v g_u] = 0, \tag{6.28}$$

with roots

$$\lambda(0)_\pm = \frac{(f_u + g_v) \pm \sqrt{(f_u + g_v)^2 - 4(f_u g_v - f_v g_u)}}{2}. \tag{6.29}$$

Insisting that $\Re e(\lambda(0)) < 0$ gives the conditions

$$f_u + g_v \;<\; 0, \tag{6.30}$$

$$f_u g_v - f_v g_u \;>\; 0. \tag{6.31}$$

6.2.2 Instability with diffusion

Now consider the effects of diffusion. In addition to $\Re e(\lambda(0)) < 0$, we must show, for diffusion-driven instability, that there exists $k^2 \neq 0$ such that

$$\Re e(\lambda(k^2)) > 0, \tag{6.32}$$

so that diffusion does indeed drive an instability.

We have that $\lambda(k^2)$ satisfies

$$\lambda^2 + \left[(D_u + D_v)k^2 - (f_u + g_v)\right]\lambda + h(k^2) = 0, \tag{6.33}$$

where

$$h(k^2) = D_u D_v k^4 - (D_v f_u + D_u g_v)k^2 + (f_u g_v - g_u f_v), \tag{6.34}$$

and

$$\alpha = (f_u + g_v) - (D_u + D_v)k^2 < 0. \tag{6.35}$$

Thus $\Re e(\lambda(k^2)) > 0$ requires that

$$\Re e\left(\alpha \pm \sqrt{\alpha^2 - 4h(k^2)}\right) > 0 \quad \Longrightarrow \quad h(k^2) < 0. \tag{6.36}$$

Hence we must find k^2 such that

$$h(k^2) = D_u D_v k^4 - (D_v f_u + D_u g_v)k^2 + (f_u g_v - g_u f_v) < 0, \tag{6.37}$$

so that we have $k^2 \in [k_-^2, k_+^2]$ where $h(k_\pm^2) = 0$. Figure 6.1 shows a plot of a caricature $h(k^2)$.

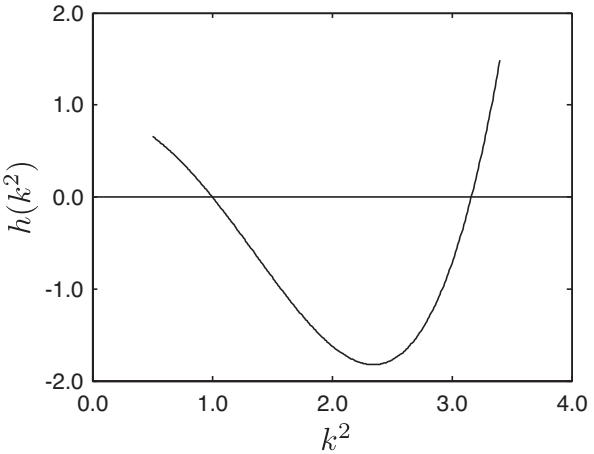

Figure 6.1: A plot of a caricature $h(k^2)$.

We conclude that we have instability whenever

$$k^2 \in \left[\frac{A - \sqrt{A^2 - B}}{2D_u D_v}, \frac{A + \sqrt{A^2 - B}}{2D_u D_v}\right] = \left[k_-^2, k_+^2\right], \tag{6.38}$$

where

$$A = D_v f_u + D_u g_v \quad \text{and} \quad B = 4D_u D_v (f_u g_v - g_u f_v) > 0, \tag{6.39}$$

and there exists a solution of the following equation

$$\nabla^2 \boldsymbol{p} + k^2 \boldsymbol{p} = 0, \quad \boldsymbol{x} \in \Omega \quad \text{and} \quad \boldsymbol{n} \cdot \nabla \boldsymbol{p} = 0. \quad \boldsymbol{x} \in \partial\Omega, \tag{6.40}$$

for k^2 in the above range.

Insisting that k is real and non-zero (we have considered the $k = 0$ case above) we have

$$A > 0 \quad \text{and} \quad A^2 - B > 0, \tag{6.41}$$

which gives us that when $\Re e(\lambda(k^2)) > 0$, the following conditions hold:

$$D_v f_u + D_u g_v > 0, \tag{6.42}$$

$$D_v f_u + D_u g_v > 2\sqrt{D_u D_v (f_u g_v - f_v g_u)}. \tag{6.43}$$

6.2.3 Summary

We have found that diffusion-driven instability can occur when conditions stated in Equations (6.30), (6.31), (6.42) and (6.43) hold. Then the instability is driven by separable solutions which solve Equation (6.18) with k^2 in the range stated in Equation (6.38).

Key point 1. Note that the constraints in Equations (6.30) and (6.42) immediately give us that $D_u \neq D_v$. Thus one cannot have a diffusion-driven instability with *identical* diffusion coefficients.

Key point 2. From the constraints in Equations (6.30), (6.31) and (6.42) the signs of the partial derivatives f_u, g_v must be such that $\boldsymbol{J}$ takes the form

$$\boldsymbol{J} = \begin{pmatrix} + & + \\ - & - \end{pmatrix} \quad \text{or} \quad \begin{pmatrix} + & - \\ + & - \end{pmatrix} \quad \text{or} \quad \begin{pmatrix} - & - \\ + & + \end{pmatrix} \quad \text{or} \quad \begin{pmatrix} - & + \\ - & + \end{pmatrix}. \tag{6.44}$$

Key point 3. A Turing instability typically occurs via *long-range inhibition and short-range activation*. In more detail, suppose

$$\boldsymbol{J} = \begin{pmatrix} + & - \\ + & - \end{pmatrix}. \tag{6.45}$$

Then we have $f_u > 0$ and $g_v < 0$ by the signs of $\boldsymbol{J}$. In this case $D_v f_u + D_u g_v > 0 \Longrightarrow D_v > D_u$. Hence the activator has a lower diffusion coefficient and spreads less quickly than the inhibitor.

6.2.4 The threshold of a Turing instability

The threshold of a Turing instability is defined such that Equation (6.23), *i.e.*

$$D_u D_v k^4 - (D_v f_u + D_u g_v)k^2 + (f_u g_v - g_u f_v) = 0,$$

has a single root, which we will denote k_c^2. This requirement is satisfied when

$$A^2 = B \quad i.e. \quad (D_v f_u + D_u g_v)^2 = 4D_u D_v (f_u g_v - g_u f_v) > 0, \tag{6.46}$$

whereupon

$$k_c^2 = \frac{A}{2D_u D_v} = \frac{D_v f_u + D_u g_v}{2D_u D_v}. \tag{6.47}$$

Strictly one also requires that a solution exists for

$$\nabla^2 \mathbf{p} + k^2 \boldsymbol{p} = 0, \quad \boldsymbol{x} \in \Omega \quad \text{and} \quad \boldsymbol{n} \cdot \nabla \boldsymbol{p} = 0, \quad \boldsymbol{x} \in \partial\Omega, \tag{6.48}$$

when $k^2 = k_c^2$. However, the above value of k_c^2 is typically an excellent approximation.

6.3 Extended example 1

Consider the one-dimensional case

$$\frac{\partial u}{\partial t} = D_u \frac{\partial^2 u}{\partial x^2} + f(u, v), \tag{6.49}$$

$$\frac{\partial v}{\partial t} = D_v \frac{\partial^2 v}{\partial x^2} + g(u, v), \tag{6.50}$$

for $x \in [0, L]$, $t \in [0, \infty)$ and zero flux boundary conditions at $x = 0$ and $x = L$.

The analogue of

$$\nabla^2 \boldsymbol{p} + k^2 \boldsymbol{p} = 0, \quad \boldsymbol{x} \in \Omega \quad \text{and} \quad \boldsymbol{n} \cdot \nabla \boldsymbol{p} = 0, \quad \boldsymbol{x} \in \partial\Omega, \tag{6.51}$$

is

$$\frac{\mathrm{d}^2 p}{\mathrm{d}x^2} + k^2 p = 0, \quad x \in (0, L) \quad \text{and} \quad p'(0) = p'(L) = 0, \tag{6.52}$$

which gives us that

$$p_k(x) = A_k \cos(kx), \quad k = \frac{n\pi}{L}, \quad n \in \{1, 2, \ldots\}, \tag{6.53}$$

where A_k is k-dependent in general but independent of x and t.

Thus the separable solution is of the form

$$\sum_k A_k e^{\lambda(k^2)t} \cos(kx), \tag{6.54}$$

where the sum is over the allowed values of k *i.e.*

$$k = \frac{n\pi}{L}, \quad n \in \{1, 2, \ldots\}. \tag{6.55}$$

Figure 6.2 shows example patterns formed using the Gierer-Meinhardt model [4].

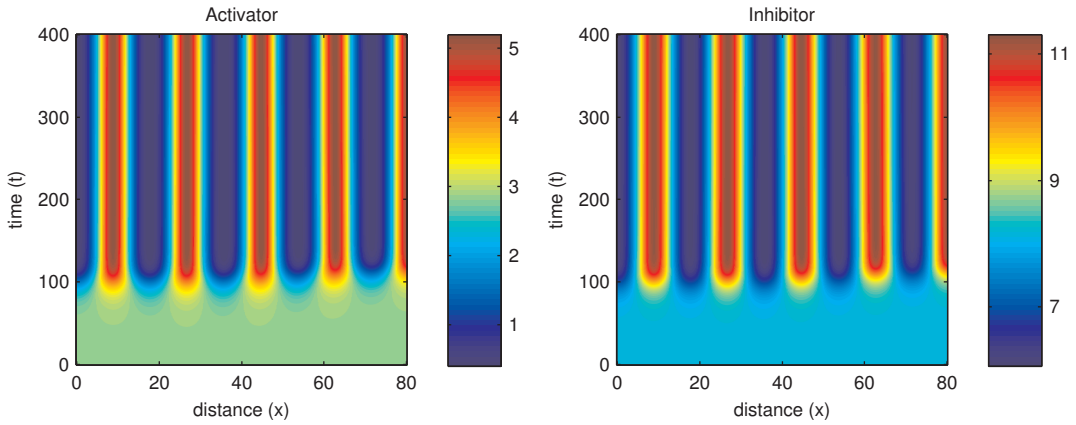

Figure 6.2: Numerical simulation of the Gierer-Meinhardt model for pattern formation.

6.3.1 The influence of domain size

If the smallest allowed value of $k^2 = \pi^2/L^2$ is such that

$$k^2 = \frac{\pi^2}{L^2} > \frac{A + \sqrt{A^2 - B}}{2D_u D_v} = k_+^2, \tag{6.56}$$

then we cannot have a Turing instability.

Thus for very small domains there is *no* pattern formation via a Turing mechanism. However, if one slowly increases the size of the domain, then L increases and the above constraint eventually breaks down and the homogeneous steady state destabilises leading to spatial heterogeneity. This phenomenon has been observed in chemical systems. It is regularly hypothesised to be present in biological systems (*e.g.* animal coat markings, fish markings, the interaction of gene products at a cellular level, the formation of ecological patchiness) though the evidence is not conclusive at the current time.

6.4 Extended example 2

Consider the two-dimensional case with spatial coordinates $\boldsymbol{x} = (x, y)^T$, $x \in [0, L_x]$, $y \in [0, L_y]$, and zero flux boundary conditions. We find that the allowed values of k^2 are

$$k^2_{m,n} = \left[\frac{m^2\pi^2}{L_x^2} + \frac{n^2\pi^2}{L_y^2} \right], \tag{6.57}$$

with

$$p_{m,n}(\boldsymbol{x}) = A_{m,n} \cos\left(\frac{m\pi x}{L_x}\right) \cos\left(\frac{n\pi y}{L_y}\right), \quad n, m \in \{0, 1, 2, \ldots\}, \tag{6.58}$$

excluding the case where n, m are both zero.

Suppose the domain is long and thin, $L_y \ll L_x$. We may have a Turing instability if

$$k^2_{m,n} = \left[\frac{m^2\pi^2}{L_x^2} + \frac{n^2\pi^2}{L_y^2} \right] \in \left[k^2_-, k^2_+\right] \quad \text{where} \quad h(k^2_\pm) = 0. \tag{6.59}$$

For L_y sufficiently small, this requires $n = 0$ and therefore no spatial variation in the y direction. This means that the seed for pattern formation predicted by the linear analysis is a separable solution which is "stripes"; this typically invokes a striped pattern once the non-linear dynamics sets in.

On the other hand, for a large rectangular domain, $L_x \sim L_y$ sufficiently large, it is clear that a Turing instability can be initiated with n, $m > 0$. This means that the seed for pattern formation predicted by the linear analysis is a separable solution which is "spots". This typically invokes a spotted pattern once the non-linear dynamics sets in.

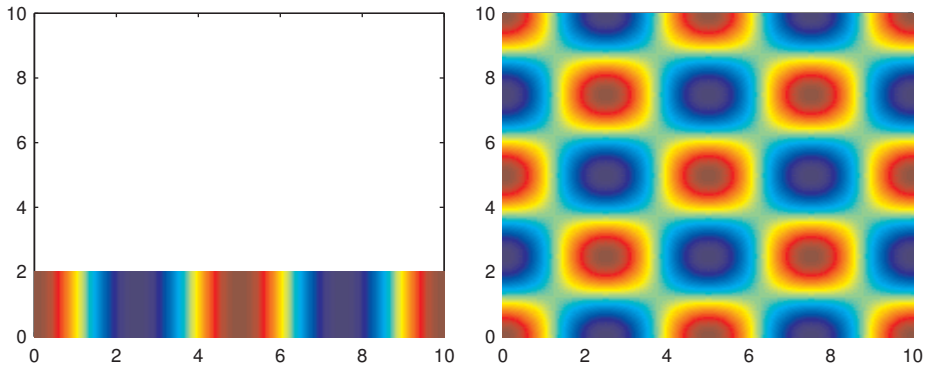

Figure 6.3: Changes in patterning as the domain shape changes.

Figure 6.3 shows how domain size may affect the patterns formed. On the left-hand side the domain is long and thin and only a striped pattern results, whilst the on the right-hand side the domain is large enough to admit patterning in both directions.

Suppose we have a domain which changes its aspect ratio from long and wide to long and thin. Then we have the following possibilities:

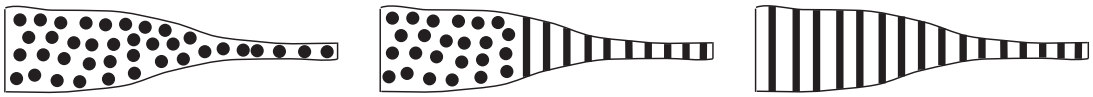

This leads to an interesting prediction, in the context of animal coat markings, that if patterning is indeed driven by a diffusion-driven instability, then one should not expect to see an animal with a striped body and a spotted tail.

Figure 6.4: Animal coat markings which are consistent with the predictions of pattern formation by a Turing instability.

Common observation is consistent with such a prediction (see Figure 6.4) but one should not expect universal laws in the realms of biology as one does in physics (see Figure 6.5). More generally, this analysis has applications in modelling numerous chemical and biochemical reactions, in vibrating plate theory, and studies of patchiness in ecology and modelling gene interactions.

Figure 6.5: Animal coat markings which are inconsistent with the predictions of pattern formation by a Turing instability.

Suggested reading.

- J. D. Murray, *Mathematical Biology, Volume II* – Chapters 2 and 3.
- N. F. Britton, *Essential Mathematical Biology* – Chapter 7.

Chapter 7

Moving boundary problems in biology

Free boundary problems have a long history of study in mathematics, and traditionally most applications have come from physics and engineering. However, there are also a number of biological scenarios that involve moving / free boundaries, in particular in the context of biological tissues which grow, develop and can be subject to a range of pathologies. Key examples include, but are not limited to, tumour growth, wound healing, tissue engineering and biofilms.

In this chapter we will focus on *in vitro* models for tumour growth. Common experimental assays involve culturing tumour cells as two-dimensional monolayers or as three-dimensional multicellular spheroids (see Figure 7.1). It is important to study the growth of monolayers and multicellular spheroids because they mimic the early stages of tumour growth, before the tumour has developed a blood supply. During this growth phase, tumour cells aggregate to form a mass which increases in size as the cells proliferate, with their growth and survival depending on local levels of vital nutrients (*e.g.* oxygen, glucose) that diffuse through the tissue. In addition, when developing and testing potential new drugs and treatments in the laboratory, experimentalists need an system which is reliable, safe and reproducible: in the context of cancer, *in vitro* models for tumour growth provide just this.

In order to model tumour growth we need to be able to predict nutrient concentration within the tumour (this determines how the tumour grows and will ultimately enable us to determine the position of the outer tumour boundary). As the tumour grows (or shrinks) the domain on which we will solve for the nutrient concentration changes – this is an example of a moving boundary problem.

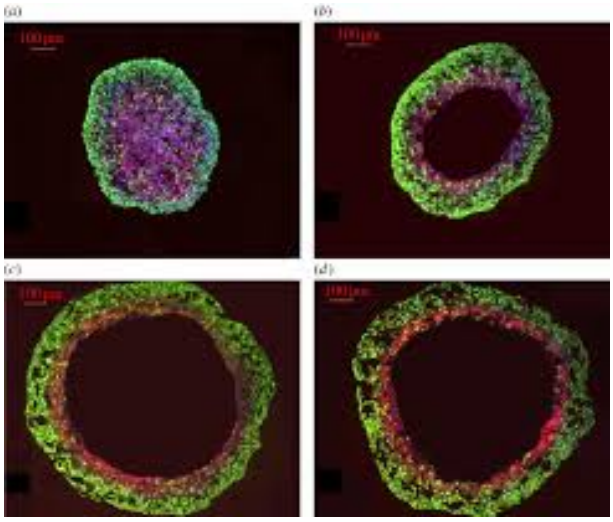

Figure 7.1: Series of images showing how the size and structure of multicellular tumour spheroids change over time.

7.1 A simple model of one-dimensional tumour growth

Consider a three-dimensional slab of tumour cells in which the cells are uniform in the y and z directions and $x = \pm R(t)$ denotes the position of the outer tissue boundary (see Figure 7.2). We would like to derive an equation for the nutrient concentration, $C(x,t)$, and suitable boundary conditions. For moving boundary problems, since the position of the boundary is unknown, we will need an extra condition to determine it. This will come from assumptions about how the tumour grows in response to consumption of nutrients.

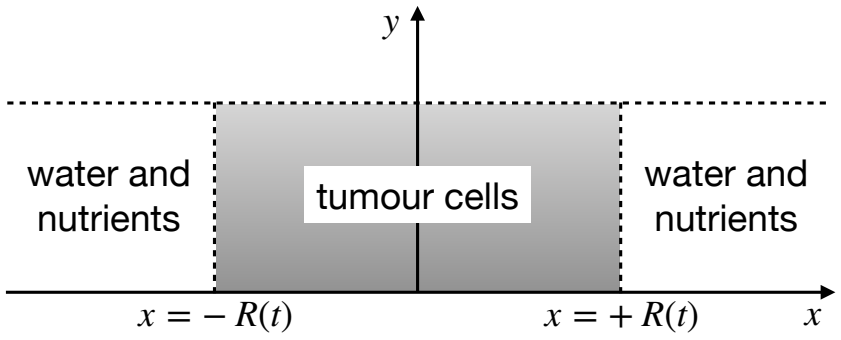

Figure 7.2: Schematic diagram of the one-dimensional tumour we will consider.

7.1.1 Nutrient concentration, $C(x,t)$

We assume that the nutrient diffuses and is consumed by tumour cells at a constant rate. Thus, $C(x,t)$ satisfies

$$\frac{\partial C}{\partial t} = D\frac{\partial^2 C}{\partial x^2} - \lambda \quad \text{for } |x| < R(t) \quad \text{(within the tumour)}, \tag{7.1}$$

where $D > 0$ is the diffusion constant and $\lambda > 0$ is the constant rate at which tumour cells consume nutrient. We assume that outside the tumour the nutrient is constantly replenished, so its concentration there is maintained at a constant value:

$$C(x,t) \equiv C^* \quad \text{for } |x| > R(t). \tag{7.2}$$

We assume that the tumour is symmetric about $x = 0$, so we only need solve on $0 \leq x \leq R(t)$, with boundary conditions

$$\frac{\partial C}{\partial x} = 0 \quad \text{at } x = 0, \tag{7.3}$$

$$C(R(t),t) = C^*. \tag{7.4}$$

We need an additional condition (or equation) that describes how tumour growth (represented by changes in $R(t)$) depends on nutrient levels.

7.1.2 Tumour boundary position, $x = R(t)$

The following equation defines how the growth of the tumour depends on the nutrient concentration:

$$\frac{\mathrm{d}R}{\mathrm{d}t} = \int_0^{R(t)} P(C)\,\mathrm{d}x, \tag{7.5}$$

where $P(C)$ represents the local proliferation rate at a given point within the tumour, and we assume that it depends only on the availability of nutrient at that point. In general, we expect $P(C)$ to be an *increasing* function of C. To close the model, we prescribe the initial position of the tumour boundary:

$$R(0) = R_0. \tag{7.6}$$

Note. Strictly speaking, we should impose initial conditions for the nutrient. However, in practice, as we explain below, it is not necessary to impose initial conditions for $C(x,t)$.

7.1.3 Model reduction

Our model of tumour growth consists of Equations (7.1)–(7.6). Before solving these equations, it is helpful to non-dimensionalise and then simplify them. We take

$$x = R_0\xi, \quad R(t) = R_0 r(\tau), \quad C(x,t) = C^* c(\xi,\tau), \quad P(C) = P_0 p(c), \quad t = \frac{\tau}{P_0}, \tag{7.7}$$

where P_0 is a typical tumour proliferation rate (*e.g.* when $C \equiv C^*$, the concentration of nutrient outside the tumour).

Equation (7.1) then becomes

$$\left(\frac{R_0^2 P_0}{D}\right)\frac{\partial c}{\partial \tau} = \frac{\partial^2 c}{\partial \xi^2} - \mu, \qquad \text{where } \mu = \frac{\lambda R_0^2}{C^* D}. \tag{7.8}$$

The coefficient $R_0^2 P_0/D$ is the ratio of the diffusion timescale, R_0^2/D, to a typical timescale for tumour proliferation, $1/P_0$. Typically, the diffusion timescale is much shorter (minutes, for a small tumour) than the proliferation timescale (tumour growth occurs over weeks) and, thus,

$$\frac{R_0^2 P_0}{D} \ll 1. \tag{7.9}$$

We can therefore neglect the time derivative in the diffusion equation and, to leading order, we obtain the following dimensionless model

$$\begin{aligned}
0 &= \frac{\partial^2 c}{\partial \xi^2} - \mu \quad \text{for } 0 \le \xi \le r(\tau), && (7.10)\\
c(\xi,\tau) &\equiv 1 \quad \text{for } \xi > r(\tau), && (7.11)\\
\frac{\partial c}{\partial \xi}(0,\tau) &= 0, && (7.12)\\
c(r(\tau),\tau) &= 1, && (7.13)\\
\frac{\mathrm{d}r}{\mathrm{d}\tau} &= \int_0^{r(\tau)} p(c)\,\mathrm{d}\xi, && (7.14)\\
r(0) &= 1. && (7.15)
\end{aligned}$$

7.1.4 Solution of the reduced model

Solving Equation (7.10) gives

$$c(\xi,\tau) = \frac{\mu \xi^2}{2} + A(\tau)\xi + B(\tau). \tag{7.16}$$

Although we have removed the explicit τ-dependence from the equation for nutrient concentration, c, the dependence of A and B on τ comes via the boundary conditions. Imposing the conditions given in Equations (7.12) and (7.13) gives

$$c(\xi,\tau) = 1 - \frac{\mu}{2}\left(r^2(\tau) - \xi^2\right). \tag{7.17}$$

The nutrient concentration, c, attains its minimum value at $\xi = 0$ where

$$c(0,\tau) = 1 - \mu r^2(\tau)/2. \tag{7.18}$$

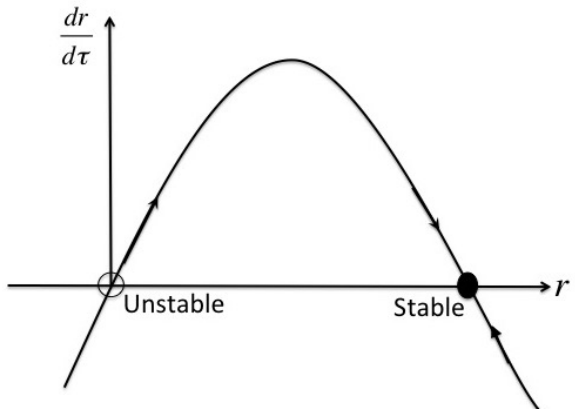

Figure 7.3: Phase-plot of $\mathrm{d}r/\mathrm{d}\tau$ versus $r(\tau)$, illustrating the steady states and their stability.

Note. As the tumour grows and $r(\tau)$ increases, the nutrient concentration at the tumour centre decreases. However, for physically realistic solutions, we require (at least) $c(0,\tau) \geq 0$.

7.1.5 Evolution of the tumour boundary, $r(\tau)$

Armed with the solution given in Equation (7.17) for the nutrient concentration, c, we can determine $r(\tau)$ via Equation (7.14). We consider the simplest case for which p is a linear function of c. A suitable nondimensionalisation of P can be chosen in order to make the coefficient of c unity, *i.e.* $p(c) = c$. Then Equation (7.14) becomes

$$\begin{aligned} \frac{\mathrm{d}r}{\mathrm{d}\tau} &= \int_0^{r(\tau)} c(\xi,\tau)\,\mathrm{d}\xi \\ &= \int_0^{r(\tau)} \left[1 - \frac{\mu}{2}\left(r^2(\tau) - \xi^2\right)\right] \mathrm{d}\xi, \end{aligned} \tag{7.19}$$

and hence

$$\frac{\mathrm{d}r}{\mathrm{d}\tau} = r(\tau)\left(1 - \frac{\mu r^2(\tau)}{3}\right) = f(r), \tag{7.20}$$

which is similar to logistic growth (indeed, $y = r^2$ undergoes logistic growth). We can integrate to find $r(\tau)$ explicitly, if required. However much information can be gained by considering the phase plane and / or carrying out linear stability analysis.

The steady states in the physically relevant regime ($r \geq 0$) are $r_1^* = 0$ and $r_2^* = \sqrt{3/\mu}$. Figure 7.3 shows the phase plane, with the steady states clearly marked. For values of r lying between $r_1^* = 0$ and $r_2^* = \sqrt{3/\mu}$, $\mathrm{d}r/\mathrm{d}t$ is positive. This means that the tumour-free state ($r_1^* = 0$) is unstable. On the other hand, perturbations about r_2^* decay over time and so the steady state is stable (if r is perturbed below r_2^* then $\mathrm{d}r/\mathrm{d}t$ is positive and r will increase until it reaches r_2^*, whereas if r is perturbed above r_2^* then $\mathrm{d}r/\mathrm{d}t$ is negative and r will decrease until it reaches r_2^*).

7.1.6 Cell death at low nutrient concentration

As nutrient levels fall the ability of a cell to proliferate and remain alive diminishes. We model these effects by assuming that there exist a threshold nutrient concentration, $c_N \in (0,1)$, such that:

- $c > c_N \implies$ cells can proliferate;
- $c < c_N \implies$ cells die and degrade (known as "necrosis").

At time $\tau = 0$, the tumour has unit radius ($r(0) = 1$), and nutrient concentration given by Equation (7.17), where we assume that

$$c(0,0) = 1 - \frac{\mu}{2} > c_N, \tag{7.21}$$

so that initially the tumour is well-nourished.

The tumour boundary evolves according to Equation (7.20) until either the steady state is attained, or until the minimum nutrient concentration is reached at the centre of the tumour, $c(0,\tau) = c_N$, and necrosis takes place there. The question is then one of which occurs first?

We determine whether necrosis occurs before the tumour attains a steady state by determining the tumour size, $r = r_1$, at which necrosis first occurs. We do this by setting $c(0,\tau) = c_N$ in Equation (7.17):

$$c_N = 1 - \frac{\mu r_1^2}{2} \quad \implies \quad r_1 = \left(\frac{2(1-c_N)}{\mu}\right)^{1/2}. \tag{7.22}$$

Noting that $r_1 < r_* = \sqrt{3/\mu}$ we see that the tumour always reaches size r_1 before the steady state is reached *i.e.* the steady state is never physically realised.

To calculate the time $\tau = \tau_1$ of necrosis onset, we separate variables and integrate Equation (7.20), between the appropriate limits:

$$\int_1^{r_1} \frac{\mathrm{d}r}{r(1-\mu r^2/3)} = \int_0^{\tau_1} \mathrm{d}\tau = \tau_1. \tag{7.23}$$

7.2 Revised model: including proliferation and necrosis

It is clear that in order to be able to describe tumour evolution after the onset of necrosis (*i.e.* for $\tau > \tau_1$), we must modify the model for $\tau > \tau_1$.

7.2.1 Model derivation for $\tau > \tau_1$

In the original model, the parameter λ in Equation (7.1) (or μ in Equation (7.10)) represents uniform nutrient uptake across the tumour. In reality, however, only live cells will absorb nutrient. Thus we replace Equation (7.10) by

$$\frac{\partial^2 c}{\partial \xi^2} = \mu H(c - c_N) \quad 0 \le \xi \le r(\tau), \quad \text{where} \quad H(c - c_N) = \begin{cases} 1 & \text{if } c > c_N, \\ 0 & \text{if } c \le c_N. \end{cases} \tag{7.24}$$

Equations (7.11), (7.12) and (7.13) are unchanged but the tumour growth equation, Equation (7.14), must be modified since only live cells proliferate and contribute to growth, while dead cells degrade and effectively remove mass from the system. Thus, again assuming proliferation (where it occurs) to be linear in c, we take

$$\frac{\mathrm{d}r}{\mathrm{d}\tau} = \int_0^{r(\tau)} p(c)\,\mathrm{d}\xi = \int_{r_N(\tau)}^{r(\tau)} c\,\mathrm{d}\xi - \int_0^{r_N(\tau)} \delta\,\mathrm{d}\xi. \tag{7.25}$$

That is, the net proliferation function $p(c)$ has the form

$$p(c) = \begin{cases} c & \text{if } c > c_N \\ -\delta & \text{if } c \le c_N, \end{cases} \tag{7.26}$$

where $\delta > 0$ is the death rate when nutrient levels are too low ($c \le c_N$) to sustain viable cells.

In summary, the full model is

$$\begin{aligned}
\frac{\partial^2 c}{\partial \xi^2} &= \mu H(c - c_N) \quad 0 \le \xi \le r(\tau), && (7.27)\\
c(\xi, \tau) &\equiv 1 \quad \xi > r(\tau), && (7.28)\\
\frac{\partial c}{\partial \xi}(0, \tau) &= 0, && (7.29)\\
c(r(\tau), \tau) &= 1, && (7.30)\\
c(r_N(\tau), \tau) &= c_N, \quad \text{with } c \text{ continuous across } \xi = r_N(\tau), && (7.31)\\
\frac{\partial c}{\partial \xi} & \quad \text{continuous across } \xi = r_N(\tau), && (7.32)\\
\frac{\mathrm{d}r}{\mathrm{d}\tau} &= \int_0^{r(\tau)} p(c)\,\mathrm{d}\xi = \int_{r_N(\tau)}^{r(\tau)} c\,\mathrm{d}\xi - \int_0^{r_N(\tau)} \delta\,\mathrm{d}\xi, && (7.33)\\
r(\tau_1) &= r_1 = \left(\frac{2(1 - c_N)}{\mu}\right)^{1/2}. && (7.34)
\end{aligned}$$

Note that for $\tau > \tau_1$, the outer moving boundary, $r(\tau)$, is determined by Equation (7.33). The edge of the necrotic region, $\xi = r_N(\tau)$, say, will also move in time: it is located where the nutrient

concentration first dips below the threshold value, $c(r_N(\tau), \tau) = c_N$. We now have two moving boundaries to determine.

7.2.2 Model solution

We solve for c in each of the two regions, noting that Equation (7.27) is equivalent to

$$\frac{\partial^2 c}{\partial \xi^2} = \begin{cases} 0 & \text{for } 0 \leq \xi \leq r_N(\tau), \\ \mu & \text{for } r_N(\tau) \leq \xi \leq r(\tau), \end{cases} \tag{7.35}$$

and hence

$$c(\xi, \tau) = \begin{cases} A_1(\tau)\xi + B_1(\tau) & \text{for } 0 \leq \xi \leq r_N(\tau), \\ \frac{\mu\xi^2}{2} + A_2(\tau)\xi + B_2(\tau) & \text{for } r_N(\tau) \leq \xi \leq r(\tau). \end{cases} \tag{7.36}$$

We fix $A_1(\tau)$ and $B_1(\tau)$ by imposing the conditions stated in Equations (7.29) and (7.31), which give

$$A_1 = 0 \quad \text{and} \quad B_1 = c_N. \tag{7.37}$$

The conditions stated in Equations (7.30), (7.31) and (7.32) supply

$$\frac{1}{2}\mu r^2(\tau) + A_2 r(\tau) + B_2 = 1, \tag{7.38}$$

$$\frac{1}{2}\mu r_N^2(\tau) + A_2 r_N(\tau) + B_2 = c_N, \tag{7.39}$$

$$\mu r_N(\tau) + A_2 = 0. \tag{7.40}$$

In this way we obtain $A_2(\tau)$ and $B_2(\tau)$ in terms of $r_N(\tau)$

$$A_2 = -\mu r_N(\tau) \quad \text{and} \quad B_2 = c_N + \frac{\mu r_N^2(\tau)}{2}, \tag{7.41}$$

and an equation relating $r_N(\tau)$ to $r(\tau)$:

$$1 - c_N = \frac{\mu}{2}\left(r(\tau) - r_N(\tau)\right)^2. \tag{7.42}$$

Equation (7.42) predicts that the width of the tumour's proliferating rim remains fixed after the onset of necrosis:

$$r(\tau) - r_N(\tau) = \sqrt{\frac{2}{\mu}(1 - c_N)} = \alpha. \tag{7.43}$$

The nutrient concentration in each region is given by

$$c(\xi,\tau) = \begin{cases} c_N & \text{for } 0 \le \xi < r_N(\tau), \\ c_N + \frac{\mu}{2}\left(\xi - r_N(\tau)\right)^2 & \text{for } r_N(\tau) \le \xi \le r(\tau), \\ 1 & \text{for } \xi > r(\tau), \end{cases} \tag{7.44}$$

with Equation (7.42) relating $r_N(\tau)$ and $r(\tau)$ and ensuring continuity of c at the tumour boundary, $r(\tau)$.

It remains to solve Equation (7.33) subject to the "initial" condition give in Equation (7.34):

$$\begin{aligned} \frac{\mathrm{d}r}{\mathrm{d}\tau} &= \int_{r_N(\tau)}^{r(\tau)} c\,\mathrm{d}\xi - \int_0^{r_N(\tau)} \delta\,\mathrm{d}\xi & (7.45)\\ &= \int_{r_N(\tau)}^{r(\tau)} \left[\frac{\mu}{2}\left(\xi - r_N(\tau)\right)^2 + c_N\right]\,\mathrm{d}\xi - \int_0^{r_N(\tau)} \delta\,\mathrm{d}\xi & (7.46)\\ &= \left(r(\tau) - r_N(\tau)\right)\left[\frac{\mu}{6}\left(r(\tau) - r_N(\tau)\right)^2 + c_N\right] - \delta r_N(\tau) & (7.47)\\ &= -\delta r(\tau) + \frac{\alpha}{3}\left(1 + 2c_N + 3\delta\right), \quad \text{with} \quad r(\tau_1) = r_1, & (7.48) \end{aligned}$$

where Equation (7.43) was used in the last line to eliminate $r_N(\tau)$. This ordinary differential equation for $r(\tau)$ is readily solved to give

$$r(\tau) = \left(r_1 - \frac{\beta}{\delta}\right) e^{-\delta(\tau-\tau_1)} + \frac{\beta}{\delta}, \qquad \beta = \frac{\alpha}{3}(1 + 2c_N + 3\delta), \tag{7.49}$$

when $\delta \neq 0$. In this case, the tumour evolves to a final dimensionless radius of β/δ.

If $\delta = 0$ (dead cells do not degrade) then we have constant growth,

$$\frac{\mathrm{d}r}{\mathrm{d}\tau} = \beta, \qquad r(\tau_1) = r_1. \tag{7.50}$$

In this case, the tumour radius does not attain a steady state: it grows linearly with τ.

7.3 Summary

Processes such as tissue growth can give rise to moving boundaries in mathematical models. In this chapter we considered simple models for tumour growth in which domain growth is driven entirely by nutrient consumption. As a result, we also needed to account for nutrient transport and uptake within the domain. As the timescale for tumour growth is typically much longer than the timescale for nutrient diffusion we were able to consider the a simplified model in which the diffusion equation is quasi-steady. We showed that, for a simple one-dimensional model

with symmetry about the ξ-axis, uniform nutrient concentration outside the tumour, and a cell proliferation rate that is linear in c, we can obtain an ordinary differential equation for the position of the tumour boundary $r(\tau)$. We demonstrated that this model is breaks down for large times because the nutrient concentration at the centre of the tumour becomes negative (before the steady state can be attained). To tackle this issue, we modified the model to allow cells to die when insufficient nutrient, $c < c_N$, is available. This modification lead to a model with two moving boundaries: the edge of the tumour (fixed by the proliferation condition) and edge of necrotic core (fixed by the condition $c = c_N$). Finally, we showed that if dead cells degrade then the new model leads to a steady state for the tumour, and otherwise linear growth ensues. There are many ways in which we could make the model more realistic, for example, we could solve in three-dimensional geometry. In addition, we could incorporate the effects of an externally-supplied drug (*e.g.* chemotherapy).

Suggested reading.

- H. P. Greenspan (1972). Models for the growth of a solid tumour by diffusion. *Stud. Appl. Math.* 52:317–344.
- A. Friedman (2015). Free boundary problems in biology. *Phil. Trans. R. Soc. A* 373:20140368.
- D. S. Jones and B. D. Sleeman (2004). *Differential Equations and Mathematical Biology,* (Taylor and Francis).

Chapter 8

From discrete to continuum models

The differential equation models we have studied thus far typically view species as densities or concentrations that vary continuously with time and position (see Figure 8.1). We have mostly used phenomenological descriptions of *e.g.* rates and forms of growth, reactions / interactions and movement to model how population density or concentration evolves in time. However, it is very difficult to relate these phenomenological "population-level" functions to the behaviour of individuals – for example, cells, animals, people, and even molecules – within the population. In fact, in writing down a model one should ideally start with a hypothesis of how the individuals behave and use mathematical techniques (*e.g.* coarse graining) to derive how these behaviours manifest at the population level. This question of how to derive differential equation models from individual-level descriptions of behaviours is the subject of this chapter. Some of the approaches that we will use to derive continuum descriptions for the case studies are explored in more detail in the Part B course *Stochastic modelling of biological systems.*

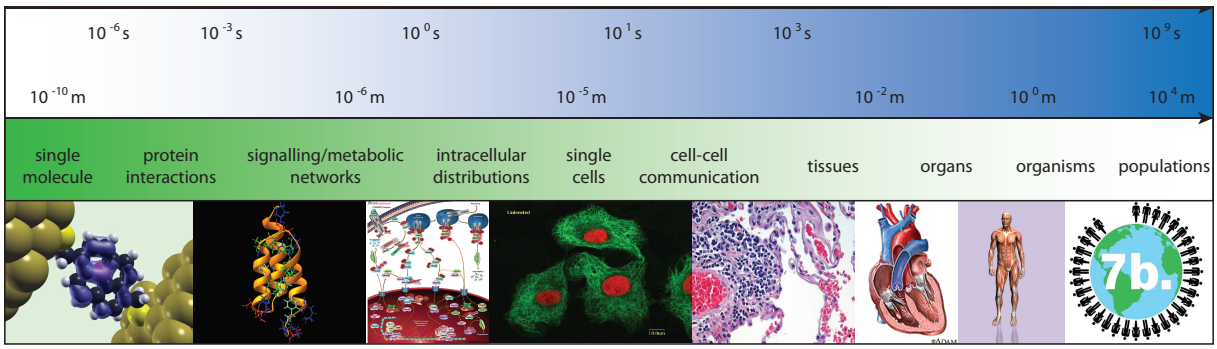

Figure 8.1: An illustration of the different spatial and temporal scales in biology.

8.1 Individual-based models for population growth

First, we will think about models for population growth, and show how to derive some of the population-level growth models that you might have seen in the Part A "Mathematical modelling in biology" course.

8.1.1 An exponential growth model

We will use the notation $p_n(t)$ to denote the probability that there are n individuals at time t, given N_0 individuals at time zero. We will assume that individuals proliferate (*i.e.* produce a daughter individual) at constant rate b, so that over a time interval of length $\mathrm{d}t$, the probability that an agent proliferates is $b\mathrm{d}t + \mathcal{O}(\mathrm{d}t^2)$. Then we can write the following discrete conservation equations

$$p_n(t+\mathrm{d}t) = (n-1)b\mathrm{d}t\, p_{n-1}(t) + (1-nb\mathrm{d}t)\, p_n(t), \quad n = N_0+1, N_0+2, \ldots, \tag{8.1}$$

and

$$p_{N_0}(t+\mathrm{d}t) = (1-N_0 b\mathrm{d}t)\, p_{N_0}(t), \tag{8.2}$$

Rearranging and dividing by $\mathrm{d}t$ gives

$$\frac{p_n(t+\mathrm{d}t) - p_n(t)}{\mathrm{d}t} = (n-1)b\, p_{n-1}(t) + nb\, p_n(t), \quad n = N_0+1, N_0+2, \ldots, \tag{8.3}$$

and

$$\frac{p_{N_0}(t+\mathrm{d}t) - p_{N_0}(t)}{\mathrm{d}t} = N_0 b\, p_{N_0}(t), \tag{8.4}$$

Taking the limit as $\mathrm{d}t \to 0$ gives

$$\frac{\mathrm{d}p_n(t)}{\mathrm{d}t} = (n-1)b\, p_{n-1}(t) + nb\, p_n(t), \quad n = N_0+1, N_0+2, \ldots, \tag{8.5}$$

and

$$\frac{\mathrm{d}p_{N_0}(t)}{\mathrm{d}t} = -N_0 b\, p_{N_0}(t), \tag{8.6}$$

with initial conditions

$$p_n(0) = \begin{cases} 1 & \text{for } n = N_0, \\ 0 & \text{for } n \neq N_0. \end{cases} \tag{8.7}$$

Note that we often call Equations (8.5)-(8.6) together the "master equation" — it is a continuous differential equation in time, t, but a discrete difference equation in n.

There are a number of ways we can use Equations (8.5)-(8.7) to gain insight into the dynamics of the system. We will briefly outline some of them below.

Evolution of the moments

To examine the mean behaviour of the system, we multiply Equations (8.5)-(8.6) by n and sum:

$$\begin{aligned}
\frac{\mathrm{d}}{\mathrm{d}t}\sum_{n=0}^{\infty} np_n(t) &= b\sum_{n=0}^{\infty} n(n-1)p_{n-1}(t) - b\sum_{n=0}^{\infty} n^2 p_n(t) && (8.8)\\
&= b\sum_{n=0}^{\infty} n(n+1)p_n(t) - b\sum_{n=0}^{\infty} n^2 p_n(t) && (8.9)\\
&= b\sum_{n=0}^{\infty} np_n(t), && (8.10)
\end{aligned}$$

where we have used $p_n(t) = 0$ for $n < N_0$, and shifted indices on the second line. Denote the mean agent number, $\langle n(t)\rangle = \sum_{n=0}^{\infty} np_n(t)$, as $M(t)$ we have

$$\frac{\mathrm{d}M}{\mathrm{d}t} = bM(t) \quad \Longrightarrow \quad M(t) = N_0 e^{bt}, \tag{8.11}$$

i.e. the population grows exponentially at rate b.

To evaluate the variance, we first derive an expression for the rate of change of $\langle n^2(t)\rangle = \sum_{n=0}^{\infty} n^2 p_n(t)$:

$$\begin{aligned}
\frac{\mathrm{d}}{\mathrm{d}t}\sum_{n=0}^{\infty} n^2 p_n(t) &= b\sum_{n=0}^{\infty} n^2(n-1)p_{n-1}(t) - b\sum_{n=0}^{\infty} n^3 p_n(t) && (8.12)\\
&= b\sum_{n=0}^{\infty} n(n+1)^2 p_n(t) - b\sum_{n=0}^{\infty} n_n^p(t) && (8.13)\\
&= b\sum_{n=0}^{\infty} (2n^2+n)p_n(t). && (8.14)
\end{aligned}$$

Using the fact that $V(t) = \langle n^2(t)\rangle - M(t)^2$, we have

$$\frac{\mathrm{d}}{\mathrm{d}t}V(t) = 2bV + bM \qquad \Longrightarrow \qquad V(t) = N_0\left(e^{bt}-1\right)e^{bt}. \tag{8.15}$$

Note. The expression for the mean population growth, Equation (8.11), is the consistent with the continuum model we would have assumed from writing population growth as the "reaction" A $\to$ 2A and using the Law of Mass Action. However, in general this will not be the case, as subsequent examples will show, and we will need to use some approximations to write down closed form equations for evolution of the mean number of individuals over time.

Generating functions

Another means to explore these types of models is the use of generating functions. We define the probability generating function $G : [-1, 1] \times [0, \infty) \to \mathbb{R}$ by

$$G(s,t) = \sum_{n=0}^{\infty} p_n(t) s^n.$$

Recall that we can recover a number of useful statistics about the $p_n(t)$ by evaluating the generating function in different ways. For example, the coefficient of s^n is $p_n(t)$ and

$$M(t) = \frac{\partial G}{\partial s}(1,t), \tag{8.16}$$

$$V(t) = \frac{\partial^2 G}{\partial s^2}(1,t) + M(t) - M^2(t). \tag{8.17}$$

To make progress, we multiply Equations (8.5)-(8.6) by s^n, sum over n and shift indices to give a partial differential equation for $G(s,t)$:

$$\begin{aligned}
\frac{\partial G}{\partial t} &= \frac{\partial}{\partial t} \sum_{n=0}^{\infty} p_n(t) s^n \\
&= b \left[\sum_{n=0}^{\infty} (n-1) p_{n-1}(t) s^n - \sum_{n=0}^{\infty} n p_n(t) s^n \right] \\
&= b \left[\sum_{n=0}^{\infty} n p_n(t) s^{n+1} - \sum_{n=0}^{\infty} n p_n(t) s^n \right] \\
&= b \left[s^2 \sum_{n=0}^{\infty} n p_n(t) z^{n-1} - s \sum_{n=0}^{\infty} n p_n(t) s^{n-1} \right] \\
&= bs(s-1) \frac{\partial G}{\partial s}.
\end{aligned} \tag{8.18}$$

We then need to solve

$$\frac{\partial G}{\partial t} = bs(s-1) \frac{\partial G}{\partial s} \quad \text{with} \quad G(s,0) = s^{N_0}. \tag{8.19}$$

The characteristic equations are

$$\frac{\mathrm{d}t}{\mathrm{d}\tau} = 1, \quad \frac{\mathrm{d}s}{\mathrm{d}\tau} = -bs(s-1), \quad \frac{\mathrm{d}G}{\mathrm{d}\tau} = 0, \tag{8.20}$$

with

$$t(z,0) = 0, \quad s(z,0) = z, \quad G(z,0) = z^{N_0}, \qquad |z| \leq 1. \tag{8.21}$$

We can integrate the first and third of these to give

$$t(z,\tau) = \tau \qquad \text{and} \qquad G(z,\tau) = z^{N_0}. \tag{8.22}$$

We can use partial fractions to integrate the second: we have

$$-b\tau + B(z) = \int \left(\frac{1}{s-1} - \frac{1}{s}\right) \mathrm{d}s = \ln\left(\frac{s-1}{s}\right), \tag{8.23}$$

where

$$B(s) = \ln\left(\frac{s-1}{s}\right). \tag{8.24}$$

This gives

$$s = \frac{z}{z-(z-1)e^{b\tau}}, \tag{8.25}$$

and hence

$$G(s,t) = \left(\frac{s}{s-(s-1)e^{bt}}\right)^{N_0} = \left(\frac{se^{-bt}}{1-(1-e^{-bt})s}\right)^{N_0}. \tag{8.26}$$

Note that this formulation reveals that $G(s,t)$ is the probability generating function of a negative binomial distribution *i.e.* that the $p_n(t)$ are negative-binomial distributed, $p_n(t) \sim \mathrm{NB}(N,p)$ with parameters $p = e^{-bt}$ and $N = N_0$.

The mean is given by

$$M(t) = \left.\frac{\partial G}{\partial s}\right|_{s=1} = N_0 e^{bt}, \tag{8.27}$$

and the variance is

$$V(t) = \left.\frac{\partial^2 G}{\partial s^2}\right|_{s=1} + \left.\frac{\partial G}{\partial s}\right|_{s=1} - \left(\left.\frac{\partial G}{\partial s}\right|_{s=1}\right)^2 = N_0\left(e^{bt}-1\right)e^{bt}. \tag{8.28}$$

More generally, we can evaluate $p_n(t)$ (for any n) via differentiation of the result in Equation (8.26).

8.1.2 Models for stochastic logistic growth

We will now consider a population of individuals for which, when there are n individuals in the population, the probability a single individual is born over a time interval of length $\mathrm{d}t$ is $\lambda_n \mathrm{d}t + \mathcal{O}(\mathrm{d}t^2)$, and the probability that a single individual dies over a time interval of length $\mathrm{d}t$ is $\mu_n \mathrm{d}t + \mathcal{O}(\mathrm{d}t^2)$. We further assume that the probability that more than one individual is born or dies is $\mathcal{O}(\mathrm{d}t^2)$, and that there are initially N_0 individuals in the population.

Then we can write the following discrete conservation equations

$$p_n(t+\mathrm{d}t) = \lambda_{n-1}\mathrm{d}t\, p_{n-1}(t) + (1 - \lambda_n \mathrm{d}t - \mu_n \mathrm{d}t)\, p_n(t) + \mu_{n+1}\mathrm{d}t\, p_{n+1}(t), \quad n = 0, 1, 2, \ldots, \tag{8.29}$$

with

$$p_{-1}(t) \equiv 0. \tag{8.30}$$

Note that from a biological perspective it is sensible to assume that $\mu_0 = 0$ so that there are no deaths when the population contains zero individuals.

Rearranging, dividing by $\mathrm{d}t$ and taking the limit as $\mathrm{d}t \to 0$ gives

$$\frac{\mathrm{d}p_n(t)}{\mathrm{d}t} = \lambda_{n-1}p_{n-1}(t) - (\lambda_n + \mu_n)p_n(t) + \mu_{n+1}p_{n+1}(t), \quad n = 0, 1, 2, \ldots, \tag{8.31}$$

with

$$p_{-1}(t) \equiv 0, \tag{8.32}$$

and initial conditions

$$p_n(0) = \begin{cases} 1 & \text{for } n = N_0, \\ 0 & \text{for } n \neq N_0. \end{cases} \tag{8.33}$$

Evolution of the mean number of individuals

To examine the mean behaviour of the system, we multiply Equations (8.31) by n and sum:

$$\begin{aligned} \frac{\mathrm{d}}{\mathrm{d}t}\sum_{n=0}^{\infty} np_n(t) &= \sum_{n=0}^{\infty} n\lambda_{n-1}p_{n-1}(t) - \sum_{n=0}^{\infty} n(\lambda_n + \mu_n)p_n(t) + \sum_{n=0}^{\infty} n\mu_{n+1}p_{n+1}(t) \\ &= \sum_{n=0}^{\infty}(n+1)\lambda_n p_n(t) - \sum_{n=0}^{\infty} n(\lambda_n + \mu_n)p_n(t) + \sum_{n=0}^{\infty}(n-1)\mu_n p_n(t) \\ &= \sum_{n=0}^{\infty}\lambda_n p_n(t) - \sum_{n=0}^{\infty}\mu_n p_n(t). \end{aligned} \tag{8.34}$$

We now make the assumption that

$$\lambda_n = \begin{cases} b_1 n + b_2 n^2 & \text{for } n > 0, \\ 0 & \text{for } n = 0, \end{cases} \qquad \text{and} \qquad \mu_n = \begin{cases} d_1 n + d_2 n^2 & \text{for } n > 0, \\ 0 & \text{for } n = 0, \end{cases} \tag{8.35}$$

where b_1, b_2, d_1 and d_2 are non-negative constants. In this case, we have

$$\frac{\mathrm{d}M}{\mathrm{d}t} = (b_1 - d_1)M + (b_2 - d_2)\langle n^2 \rangle, \tag{8.36}$$

where the second moment is defined as

$$\langle n^2 \rangle = \sum_{n=0}^{\infty} n^2 p_n(t). \tag{8.37}$$

Note that the presence of the $\langle n^2 \rangle$ term means that Equation (8.36) is not closed so we cannot immediately solve it to provide insight into how the mean number of individuals evolves over time. In order to make progress, we invoke a commonly used mean-field assumption of the form $\langle n^2 \rangle \approx M^2$ to write

$$\frac{\mathrm{d}M}{\mathrm{d}t} = (b_1 - d_1)M + (b_2 - d_2)M^2 = rM\left(1 - \frac{M}{K}\right), \tag{8.38}$$

where

$$r = b_1 - d_1 \qquad \text{and} \qquad K = \frac{b_1 - d_1}{d_2 - b_2}. \tag{8.39}$$

Hence, the mean number of individuals approximately evolves according to the logistic equation, and we can solve explicitly to find $M(t)$. However, note that there are four constants in the individual-level model, but only two in the deterministic model. Comparing the coefficients, we see that there are an infinite number of stochastic models that all give rise, approximately, to the same average behaviour.

Evolution of the second moment

Instead of closing at first order using the mean-field assumption, we can derive an expression for how the second moment evolves over time:

$$\begin{aligned}
\frac{\mathrm{d}}{\mathrm{d}t}\langle n^2 \rangle &= \frac{\mathrm{d}}{\mathrm{d}t}\sum_{n=0}^{\infty} n^2 p_n(t) \\
&= \sum_{n=0}^{\infty} n^2 \lambda_{n-1} p_{n-1}(t) - \sum_{n=0}^{\infty} n^2(\lambda_n + \mu_n)p_n(t) + \sum_{n=0}^{\infty} n^2 \mu_{n+1} p_{n+1}(t) \qquad (8.40) \\
&= \sum_{n=0}^{\infty} (n+1)^2 \lambda_n p_n(t) - \sum_{n=0}^{\infty} n^2(\lambda_n + \mu_n)p_n(t) + \sum_{n=0}^{\infty} (n-1)^2 \mu_n p_n(t) \\
&= \sum_{n=0}^{\infty} (2n+1)\lambda_n p_n(t) - \sum_{n=0}^{\infty} (2n-1)\mu_n p_n(t). \qquad (8.41)
\end{aligned}$$

For the specific choices of λ_n and μ_n we made above, we have

$$\frac{\mathrm{d}}{\mathrm{d}t}\langle n^2 \rangle = (b_1 + d_1)M + \{2(b_1 - d_1) + (b_2 + d_2)\}\langle n^2 \rangle + 2(b_2 - d_2)\langle n^3 \rangle. \tag{8.42}$$

We make two observations. First, there are distinct four parameter combinations in Equation (8.42): $b_1 - d_1$, $b_1 + d_1$, $b_2 - d_2$ and $b_2 + d_2$. This means that we could potentially use the variability in population numbers to differentiate between models that display the same averaged behaviour. Second, the variance increases as $b_1 + d_1$ and $b_2 + d_2$ are increased.

Finally, we remark that Equation (8.42) is, similarly to the equation for $M(t)$, not closed. To find an approximate solution we would need to make a further closure assumption to write $\langle n^3 \rangle$ in terms of M and $\langle n^2 \rangle$. This need for moment closure approximations in order to find closed form expressions for the mean and variance of the number of individuals arises whenever λ_n and/or μ_n are quadratic or higher order polynomials in n. The most appropriate closure assumption, for a general scenario, is still an open question.

8.2 Individual-based models for cell motility

In this section we will write down some simple models for the behaviour of motile cell populations, and learn how to coarse grain them to derive corresponding partial differential equation models for the evolution of cell density. For simplicity, we will assume that each cell undergoes a random walk on a lattice in one spatial dimension. However it is simple to extend all these models to two and three spatial dimensions.

8.2.1 A simple model of biased cell motility

We first consider single cell undergoing a random walk on one-dimensional lattice along the x-axis, where the lattice sites are all of width $\mathrm{d}x$ (see Figure 8.2). We let $p_n(t)$ now be the probability that the cell is in lattice site n at time t, with $p_n(0) = p_n^0$ *i.e.* the probability that the particle is initially at site n is p_n^0 for $n \in \mathbb{Z}$.

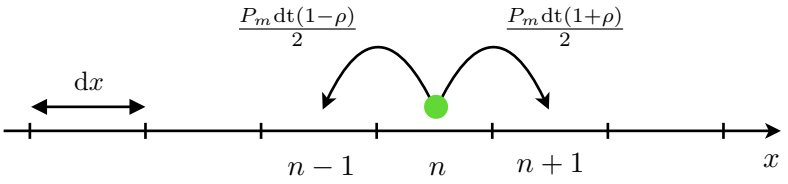

Figure 8.2: Illustration of the biased random walk in one dimension.

We assume that over a time step of length $\mathrm{d}t$, the cell moves one lattice site to the right with constant probability $P_m(1 + \rho)\mathrm{d}t/2$, or one lattice site to the left with constant probability $P_m(1 - \rho)\mathrm{d}t/2$ (see Figure 8.2). Note that this equates to an overall movement rate of P_m (and probability of movement $P_m \mathrm{d}t$), with movements biased in the right-hand direction for $\rho > 0$.

We can write down a discrete conservation equation for the position of the cell at time $t + \mathrm{d}t$:

$$p_n(t + \mathrm{d}t) = \frac{1}{2}(1 + \rho)P_m \mathrm{d}t\, p_{n-1}(t) - (1 - P_m \mathrm{d}t)\, p_n(t) + \frac{1}{2}(1 - \rho)P_m \mathrm{d}t\, p_{n+1}(t). \tag{8.43}$$

If the size of the lattice is sufficiently small we can relate $p_n(t)$ to a continuous probability $p(x, t)$ by writing $p_n(t) = p(n\mathrm{d}x, t)$, and then rearrange Equation (8.43) to give

$$\frac{p(n\mathrm{d}x, t + \mathrm{d}t) - p(n\mathrm{d}x, t)}{\mathrm{d}t} = \frac{1}{2}(1+\rho)P_m\, p((n-1)\mathrm{d}x, t) - P_m p(n\mathrm{d}x, t) + \frac{1}{2}(1-\rho)P_m\, p((n+1)\mathrm{d}x, t) \tag{8.44}$$

We can then perform Taylor expansions in both $\mathrm{d}x$ and $\mathrm{d}t$ to give

$$\begin{aligned} \frac{\partial}{\partial t}p(n\mathrm{d}x, t) + \mathcal{O}(\mathrm{d}t) \quad = \quad & \left(\frac{1}{2}(1 + \rho)P_m - P_m + \frac{1}{2}(1 - \rho)P_m\right) p(n\mathrm{d}x, t) \\ & + \left(-\frac{1}{2}(1 + \rho)P_m + \frac{1}{2}(1 - \rho)P_m\right) \mathrm{d}x \frac{\partial}{\partial x} p(n\mathrm{d}x, t) \\ & + \left(\frac{1}{4}(1 + \rho)P_m + \frac{1}{2}(1 - \rho)P_m\right) \mathrm{d}x^2 \frac{\partial^2}{\partial x^2} p(n\mathrm{d}x, t) + \mathcal{O}(\mathrm{d}x^3). \end{aligned} \tag{8.45}$$

Simplifying, and taking the limit as $\mathrm{d}x$ and $\mathrm{d}t$ tend to zero, gives an advection-diffusion partial differential equation for the probability of the position of the cell:

$$\frac{\partial p}{\partial t} = D\frac{\partial^2 p}{\partial x^2} - v\frac{\partial p}{\partial x}, \tag{8.46}$$

where

$$D = \lim_{\mathrm{d}x \to 0} \frac{P_m \mathrm{d}x^2}{2} \qquad \text{and} \qquad v = \lim_{\mathrm{d}x \to 0} P_m \rho\, \mathrm{d}x. \tag{8.47}$$

The initial conditions are given as the continuous extension of the discrete initial condition: $p(x, 0) = p^0(x)$.

We now make a number of remarks about the derivation.

- If $\rho = 0$ the the jumps are unbiased, and the position of the particle evolves according to the diffusion equation.
- We can verify that our results make sense by considering the units of the parameters D and v. In SI units we have:
  - the units of P_m are s^{-1} and those of $\mathrm{d}x$ are m, hence the units of D are $\mathrm{m}^2\mathrm{s}^{-1}$;
  - the units of P_m are s^{-1}, those of $\mathrm{d}x$ are m and ρ is non-dimensional, hence the units of v are ms^{-1}.

- The bias must scale with $\mathrm{d}x$ for a well-defined limit (since P_m scales like $1/\mathrm{d}x^2$).
- Equation (8.46) can also be used to describe the evolution of a population of non-interacting cells by suitable choice of initial condition.

There are many ways to extend the basic framework used above to take more biological detail into account. The key point is to include all the relevant (source and sink) terms when using the principle of mass balance to derive the discrete conservation equations. Other processes that could be included are:

- chemotaxis – here, the probabilities of moving left and right from site n will depend on the concentration of a diffusible chemoattractant in boxes $n \pm 1$ and box n;
- proliferation and death;
- competition for space.

We consider this idea of competition for space in the next section.

8.2.2 A model of biased cell motility that includes competition for space

We now consider a population of cells undergoing a random walk on one-dimensional lattice along the x-axis, where the lattice sites are all of width $\mathrm{d}x$. We assume that $\mathrm{d}x$ is approximately equal to one cell diameter, so that at most one cell can occupy any site on the lattice at any time (see Figure 8.3).

We let $p(A_n, t)$ be the probability that a cell is in lattice site n at time t. The probability that the lattice site is empty is denoted $p(0_n, t)$ where $p(0_n, t) = 1 - p(A_n, t)$. We prescribe initial conditions of the form $p(A_n, 0) = p_n^0$ *i.e.* the probability that a cell is initially at site n is p_n^0 for $n \in \mathbb{Z}$.

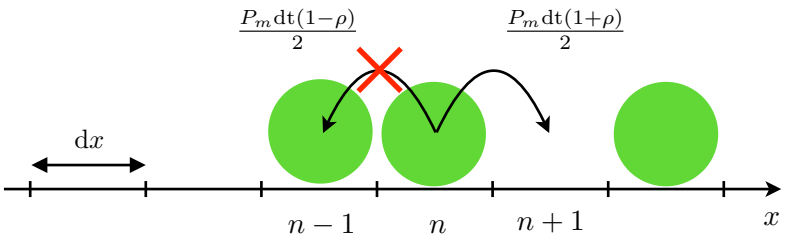

Figure 8.3: Illustration of the biased random walk with exclusion in one dimension. Note that if the cell at lattice site n attempts to jump left, the jump is aborted because there is already a cell in site $n-1$.

We assume that over a time step of length $\mathrm{d}t$, the cell attempts to move with probability $P_m\mathrm{d}t$. If the cell attempts to move, it will jump one lattice site to the right with constant probability $(1+\rho)/2$, or one lattice site to the left with constant probability $(1-\rho)/2$, but the attempted move is successful only if the target site is vacant.

We can write down a discrete conservation equation for the change in occupancy probability of lattice site n over time step $[t, t+\mathrm{d}t)$:

$$\begin{aligned} p(A_n, t+\mathrm{d}t) - p(A_n, t) &= \frac{1}{2}(1+\rho)P_m\mathrm{d}t\, p(A_{n-1}, 0_n, t) - \frac{1}{2}(1-\rho)P_m\mathrm{d}t\, p(0_{n-1}, A_n, t) \\ &\quad + \frac{1}{2}(1-\rho)P_m\mathrm{d}t\, p(0_n, A_{n+1}, t) - \frac{1}{2}(1+\rho)P_m\mathrm{d}t\, p(A_n, 0_{n+1}, t), \end{aligned} \tag{8.48}$$

where $p(A_n, 0_m)$ denotes the probability that site n is occupied and site m is vacant. To make progress in deriving a corresponding advection-diffusion partial differential equation, we write

$$\begin{aligned} p(A_n, t+\mathrm{d}t) - p(A_n, t) &= \frac{P_m}{2}\mathrm{d}t\Big[p(A_{n-1}, 0_n, t) - p(0_{n-1}, A_n, t)\Big] \\ &\quad + \frac{P_m}{2}\mathrm{d}t\Big[p(0_n, A_{n+1}, t) - p(A_n, 0_{n+1}, t)\Big] \\ &\quad + \frac{P_m}{2}\rho\,\mathrm{d}t\Big[p(A_{n-1}, 0_n, t) - p(0_{n-1}, A_n, t)\Big] \\ &\quad - \frac{P_m}{2}\rho\,\mathrm{d}t\Big[p(0_n, A_{n+1}, t) - p(A_n, 0_{n+1}, t)\Big]. \end{aligned} \tag{8.49}$$

We now divide by $\mathrm{d}t$ and simplify the first two terms on the right-hand side using conservation statements of the form

$$p(A_n, A_m, t) + p(A_n, 0_m, t) = p(A_n, t), \tag{8.50}$$

to give

$$\frac{P_m}{2}\Big[p(A_{n-1}, t) - 2p(A_n, t) + p(A_{n+1}, t)\Big]. \tag{8.51}$$

In order to close the system of discrete conservation equations (for $n \in \mathbb{Z}$), so that the right-hand side contains only occupancy probabilities of single lattice sites (rather than pairs of neighbouring lattice sites), we make the assumption that the occupancy probabilities of neighbouring lattice sites are independent of one another *e.g.*

$$p(A_n, 0_{n\pm1}) = p(A_n)p(0_{n\pm1}). \tag{8.52}$$

This is known as a mean-field approximation, and it allows us to write

$$\begin{aligned}\frac{p(A_n,t+\mathrm{d}t)-p(A_n,t)}{\mathrm{d}t} &= \frac{P_m}{2}\Big[p(A_{n-1},t)-2p(A_n,t)+p(A_{n+1},t)\Big]\\ &\quad+\frac{P_m}{2}\rho\Big\{\big[1-p(A_n,t)\big]\big[p(A_{n-1},t)-p(A_{n+1},t)\big]\\ &\qquad+p(A_n,t)\Big[\big(1-p(A_{n-1},t)\big)-\big(1-p(A_{n+1})\big)\Big]\Big\}. \quad (8.53)\end{aligned}$$

Similarly to the previous section, if the size of the lattice sites (and hence the cell diameter) are sufficiently small compared to the region occupied by the cell population, we can relate $p(A_n,t)$ to a continuous probability by writing (with plenty of abuse of notation!) $p(A_n,t)=p(n\mathrm{d}x,t)$ so that

$$\begin{aligned}\frac{p(n\mathrm{d}x,t+\mathrm{d}t)-p(n\mathrm{d}x,t)}{\mathrm{d}t} &= \frac{P_m}{2}\Big[p((n-1)\mathrm{d}x,t)-2p(n\mathrm{d}x,t)+p((n+1)\mathrm{d}x,t)\Big] \quad (8.54)\\ &\quad+\frac{P_m}{2}\rho\Big\{\big[1-p(n\mathrm{d}x,t)\big]\big[p((n-1)\mathrm{d}x,t)-p((n+1)\mathrm{d}x,t)\big]\\ &\qquad+p(n\mathrm{d}x,t)\Big[\big(1-p((n-1)\mathrm{d}x,t)\big)-\big(1-p((n+1)\mathrm{d}x)\big)\Big]\Big\}.\end{aligned}$$

We can then perform Taylor expansions in both $\mathrm{d}x$ and $\mathrm{d}t$, and take the limit as $\mathrm{d}x$ and $\mathrm{d}t$ tend to zero, to give an advection-diffusion partial differential equation for the cell density:

$$\frac{\partial p}{\partial t}=D\frac{\partial^2 p}{\partial x^2}-v\frac{\partial}{\partial x}\big(p(1-p)\big), \quad (8.55)$$

where

$$D=\lim_{\mathrm{d}x\to 0}\frac{P_m\mathrm{d}x^2}{2} \qquad \text{and} \qquad v=\lim_{\mathrm{d}x\to 0}P_m\rho\,\mathrm{d}x. \quad (8.56)$$

Once again, the initial conditions are given as the continuous extension of the discrete initial condition: $p(x,0)=p^0(x)$.

As in the non-excluding case if $\rho=0$ then the jumps are unbiased and the position of the particle evolves according to the diffusion equation. However, if $\rho\neq 0$, then we note two differences. First, we need to use a moment closure approximation to derive a closed form partial differential equation describing evolution of the density over time. This means that Equation (8.55) does not exactly describe how the density evolves – in particular, we might expect discrepancies whenever there are correlations in lattice site occupancies, so that $p(A_n,A_m)$ is not well approximated by $p(A_n)p(A_m)$. We also note that the inclusion of a simple description of competition for space impacts the advection term, changing it from $v\partial p/\partial x$ to $v\partial p(1-p)/\partial x$.

Suggested reading

- H. G. Othmer, S. A. Dunbar and W. Alt (1988). Models of dispersal in biological systems. *J. Math. Biol.* 26:263–298.
- L. J. S. Allen (2010). *An Introduction to Stochastic Processes With Applications in Biology.* Chapman and Hall/CRC; 2nd edition.
- S. A. H. Gertiz and E. Kisdi (2012). Mathematical ecology: why mechanistic models? *Bull. Math. Biol.* 65:1411–1415.

Bibliography

[1] J. Beam Dowd, L. Andriano, D. M. Brazel, V. Rotondi, P. Block, X. Ding, Y. Liu, and M. C. Mills (2020). Demographic science aids in understanding the spread and fatality rates of COVID-19. *Proc. Nat. Acad. Sci. USA* 117(18):9696–9698.

[2] N.F. Britton (2005). *Essential Mathematical Biology.* Springer Undergraduate Mathematics Series. Springer.

[3] L. Edelstein-Keshet (2005). *Mathematical Models in Biology.* SIAM Classics in Applied Mathematics.

[4] A. Gierer and H. Meinhardt (1972). A theory of biological pattern formation. *Kybernetik* 12: 30-39.

[5] P. Glendinning (1999). *Stability, Instability and Chaos: An Introduction to the Theory of Nonlinear Differential Equations.* Cambridge Texts in Applied Mathematics.

[6] T. Hillen and K. Painter (2009). A user's guide to PDE models for chemotaxis. *J. Math. Biol.* 58(1):183–217.

[7] D.W. Jordan and P. Smith (2002). *Mathematical Techniques: An Introduction for the Engineering, Physical and Mathematical Sciences.* Oxford University Press, 3rd edition.

[8] J. P. Keener and J. Sneyd (1998). *Mathematical Physiology,* Volume 8 of *Interdisciplinary Applied Mathematics.* Springer, New York, 1st edition.

[9] J.D. Murray (2003). *Mathematical Biology I: An Introduction,* Volume I. Springer-Verlag, 3rd edition.

[10] J.D. Murray (2003). *Mathematical Biology II: Spatial Models and Biochemical Applications,* Volume II. Springer-Verlag, 3rd edition.

[11] A. Okubo, P. K. Maini, M. H. Williamson and J. D. Murray (1989). On the spread of the grey squirrel in Great Britain. *Proc. Roy. Soc. Lond. B* 238(1291):113–125.

[12] L. E. Reichl (2009). *A Modern Course in Statistical Physics.* Wiley-VCH, 3rd edition. https://archive.org/details/L.E.ReichlAModernCourseInStatisticalPhysicsWiley1998/mode/2up

[13] D. Thomas and J. Kernevez (Eds) (1976). *Analysis and Control of Immobilized Enzyme Systems.* North-Holland, Amsterdam.

[14] A. M. Turing (1952). The chemical basis of morphogenesis. *Roy. Soc. Lond. Phil. Trans. B* 237:37–72.

[15] United Nations, Department of Economic and Social Affairs, Population Division (2017). *World Population Ageing 2017 - Highlights (ST/ESA/SER.A/397).* https://www.un.org/en/development/desa/population/publications/pdf/ageing/WPA2017_Highlights.pdf

[16] Kelvinsong — CCO, https://commons.wikimedia.org/w/index.php?curid=22965076

[17] L. Wolpert (1969). Positional information and the spatial pattern of cellular differentiation. *J. Theor. Biol.* 25(1):1–47.